DIGITAL COMPUTER SOLUTION FOR PROPAGATION OF A SPHERICAL SHOCK WAVE IN ALUMINUM

by

HARRY RUSSELL LAKE

Bachelor of Science

Oklahoma State University

1959

Submitted to the Faculty of the Graduate School of
the Oklahoma State University
in partial fulfillment of the requirements
for the degree of
MASTER OF SCIENCE
May, 1962

DIGITAL COMPUTER SOLUTION FOR PROPAGATION OF

A SPHERICAL SHOCK WAVE IN ALUMINUM

Thesis Approved:

Francis C. Todd
Thesis Adviser

William J. Lewis

Queen Machtemi
Dean of the Graduate School

PREFACE

This work was undertaken at the suggestion of Dr. F. C. Todd who acted as my adviser and project supervisor. The purpose of the paper is to study the shock wave initiated by a micrometeoroid impacting on a semi-infinite surface.

The problem for study is intended to yield an order of magnitude solution to the phenomena of micrometeoroid impact. This first solution is necessary to provide the basis for assumptions that are necessary to treat more complex problems.

The assistance and guidance of Dr. Todd have been invaluable in the completion of this work. The author is also indebted to Mr. B. A. Sodek and Mr. J. G. Ables for assistance in this work and to Mr. William Granet for consultations concerning the digital computer programming.

The work was carried out under NASA Contract Number NASr-7 administered through Research Foundation, Oklahoma State University.

TABLE OF CONTENTS

TABLE OF CONTENTS (Continued)

LIST OF TABLES

CHAPTER I

INTRODUCTION AND STATEMENT OF THE PROBLEM

Micrometeoroids are defined as particles which have a mass of less than 10^{-4} grams and velocities that range from 30,000 to 240,000 feet per second (1). They are detected by devices that are placed in high-flying rockets or satellites. One device that has been successfully used is a photomultiplier tube with a vapor deposited aluminum film covering the face. The micrometeoroids impinging upon the face of the photomultiplier are known to produce a pulse of current through the tube.

The NASA project for which this thesis is a contribution was initiated as an analytical study of micrometeoroid impact on the coated photomultiplier. The project is concerned with the mechanics of impact which result in producing light to activate the photomultiplier tube and is directed toward determining the energy, momentum and possibly the composition of the micrometeoroid from measurements on the impact.

The time interval chosen by the sponsor for this study is the first two microseconds after initiation of the impact. For purposes of reference, a typical micrometeoroid for the study has a mass of 10^{-9} grams and moves with a velocity of 36 kilometers per second. Since theoretical considerations indicate that micrometeoroids have a velocity between 30,000 and 240,000 feet

per second, the selected meteoroid has a velocity approximately midway between the extremes.

Up to this time, very few published articles have attempted to determine and analyze the impact phenomena of small particles with ultra-high velocities. One article approaches the problem from the thermal damage theory (2). In this theory, the flash of light accompanying the impact is attributed to incandescence of the target and the meteoroid in the immediate vicinity of the impact.

Bjork (16) has examined the problem of a high-velocity projectile of cylindrical symmetry impingeing upon a semi-infinite solid by a plane. His computations were intended to give an order of magnitude solution to the problem of high-velocity impact.

After consideration of a limited amount of impact data for lower velocities, a theory different from that of thermal damage has been proposed by F. C. Todd, project supervisor. This theory proposes that a plasma is formed by a strong radial shock from the impact. A plasma is defined as a mixture of ions and electrons which is expected to start to form from the applications of pressure alone at a pressure of about 100,000 atmospheres (3). The radiation that accompanies the impact results from the electrons in the plasma dropping back into their normal state, or an unfilled level after the pressure starts to decrease. This plasma theory along with other impact models is discussed in Appendix A.

The subject of this thesis is the investigation of the strong radial shock wave accompanying micrometeoroid impact. Bethe (4) has shown that propagation of a shock wave through a material may be solved provided that the equation of state for the material is known over the pressure range of the shock. Knowledge of the equation of state permits a simultaneous solution of the partial differential equations for hydrodynamic flow, which may be applied to the problem of high velocity impact. In the solution of these equations, the shock fronts are lines of discontinuity. In order to obtain a numerical solution, a pseudo-viscosity term, first introduced by J. von Neumann and R. D. Richtmyer (5), is used to smear out the shock into regions of very steep gradients.

The problem chosen for this thesis is the development of the solution of the propagation of a radial shock wave into a semi-infinite media. The reason for choosing a semi-infinite target is to simplify solving an exploratory problem. This first solution must be obtained to provide the basis for assumptions that are necessary to treat the more complex problem of a shock wave propagating into a thin film of material coating the face of a photomultiplier tube.

The work described herein may be briefly outlined as follows:

(1) An equation of state is developed for aluminum over an extended pressure range.

(2) The partial differential equations of fluid flow are developed and converted to a dimensionless form.

(3) The dimensionless hydrodynamic equations are converted to a difference equations for computer solution.

(4) The difference equations are combined with computer logic to form a FORTRAN computer program.

(5) The mechanics of developing a computer program are completed by choosing a space-time net that will give a stable solution.

(6) The computer program, combined with initial and boundary conditions, gives the solution for shock wave propagation.

CHAPTER II

SHOCK WAVE BACKGROUND THEORY

Since this thesis is to treat the shock wave initiated by a micrometeoroid impacting on a solid, it is desirable to review and develop some of the background theory necessary for the theoretical treatment of shock waves.

Historical Background

Courant and Friedrichs (6) give a brief historical background of the development of modern shock wave theory. Topics of interest from their work are presented.

In 1808, Poisson was the first to obtain a simple wave solution of the differential equation of flow on the assumption of an isothermal propagation through the gas. Forty years later in 1848 Challis noted that this equation of flow did not always give a unique solution for the flow velocity, u. The same year that Challis made his observation, Stokes proposed that, to obtain a unique solution, one should assume that a discontinuity in the velocity occurs when the velocity gradient becomes infinite. Stokes also stated that this assumed discontinuity would never exist in a physical problem since it would be smoothed out to a finite width by viscous forces. In 1858, Earnshaw developed the wave solution for the flow of gases which satisfies the relation

that the pressure is equal to a function of the density. Two years later, Riemann developed the simple wave theory solution and solved the general flow problem by using "Riemann invariants". He elaborated on the theory of shocks but made the incorrect assumption that the transition across the shock is adiabatic and reversible.

In 1869 Rankine first proposed that the transition across the shock region is a non-adiabatic process and initiated work to derive boundary conditions relating the conditions of material on either side of a shock front. In 1887, Hugoniot proved conclusively that an adiabatic reversible transition across a shock region would violate the law of conservation of energy. He also derived an equation, today known as the Hugoniot Relation, relating the change of internal energy across a shock front to the changes in pressure and density. Finally, in 1910, Rayleigh observed that entropy must increase across a shock.

Uniqueness of Solution

According to Bethe (4), a unique solution to Hugoniot's shock wave equations exists and can be found provided a complete equation of state exist for the media through which the shock propagates and provided three assumptions about the equation of state are fulfilled.

The most important condition is:

$$\left(\frac{\partial^2 P}{\partial V^2}\right)_S > 0$$

where P is the pressure, V is the specific volume, i.e., mass per unit volume, and S is the entropy. This condition is satisfied for nearly all single phase systems and is violated only for extreme cases where the pressure is smaller than 10^{-44} atmospheres.

The second and third conditions are:

$$V \left(\frac{\partial P}{\partial e}\right)_V > -2$$

and

$$\left(\frac{\partial P}{\partial V}\right)_e < 0$$

where e is the specific internal energy. The second condition is fulfilled whenever a substance expands with increasing temperature at constant pressure and is believed to be fulfilled for nearly all substances under nearly all conditions. The third condition was found to be fulfilled for all single phase systems investigated by Bethe.

Stability of Shock Waves

Shock waves, in a homogeneous medium that satisfies the necessary conditions for a unique solution, always travel with a supersonic velocity relative to a point in the material ahead of the shock and with a subsonic velocity relative to a point in the material behind the shock (7). Bethe (4) has shown that this property of a shock wave permits a simple explanation of shock

wave stability.

Consider a homogeneous medium supporting a shock wave. The stability of the shock can be examined by assuming that it starts to break up into two waves, one ahead of the other. The leading shock will travel with a supersonic velocity relative to the undisturbed material in front and with subsonic velocity relative to the material behind this leading shock but ahead of the second shock; the second shock will travel with a supersonic velocity relative to the material between the shocks since material in this region is in front of the second shock. That is, the leading shock wave travels with a subsonic velocity and the trailing shock wave travels with a supersonic velocity with respect to the material in the region between them. The trailing shock will soon overtake the leading shock and merge to form one stable wave. The same argument can be applied against a shock splitting into several waves. From these considerations, a compressive shock in a homogeneous medium, satisfying the necessary conditions for uniqueness, will be completely stable.

Rankine-Hugoniot Conditions

Shock waves are defined as dilational waves in a plastic media, or a media that has negligible resistance to shear, similar to a liquid. For this reason, the flow of the compressed media can be represented by the equations of hydrodynamic flow. In the propagation of the shock front, the pressure rises to a high value in a very thin zone which is designated as the shock front. This

very thin zone of rapidly changing pressure, density, and internal energy appears as a discontinuity in the equations for hydrodynamic flow. For a solution, it is necessary to derive conditions that relate the states of the material on one side of the shock front to those on the other side. These conditions are usually designated in the literature as the Rankine-Hugoniot conditions.

The Rankine-Hugoniot shock conditions will be derived in a simple manner on the basis of the assumption of constant flow velocity. The same conditions may be developed in a more rigorous manner from the differential equations for motion in continious flow (8).

The Rankine-Hugoniot conditions will be developed from the following laws:

(1) Conservation of Mass

(2) Conservation of Momentum

(3) Conservation of Energy

(4) Increase of entropy across the shock.

To derive the shock relations across the discontinuity, a column of gas in a tube will be considered. Assume at time, t, the column covers a length $a_o(t) \leq x \leq a_1(t)$ where $a_o(t)$ and $a_1(t)$ are the end points of the column at time, t, and x is any point in the column. Let the flow at the ends of the tube be continious. Then the following manner,

(1a) Conservation of Mass:

$$\frac{d}{dt} \int_{a_o(t)}^{a_1(t)} \rho \, dx = o$$

where ρ is the density.

(2a) Conservation of Momentum:

$$\frac{d}{dt}\int_{a_o(t)}^{a_1(t)} Pu\ dx = P(a_1,t) - P(a_o,t)$$

where u is the flow velocity and P is the pressure.

(3a) Conservation of Energy:

$$\frac{d}{dt}\int_{a_o(t)}^{a_1(t)} \rho(\tfrac{1}{2}u^2 + e)\ dx = P(a_o,t)\ u(a_o,t) - P(a_1,t)\ u(a_1,t)$$

where e is the specific internal energy.

(4a) Increase of Entropy:

$$\frac{d}{dt}\int_{a_o(t)}^{a_1(t)} \rho S\ dx \geq 0$$

where S equals the specific entropy.

Equation (2a) assumes that the only forces acting on the column are pressure forces; therefore, the time rate of change of momentum of the column equals the total resultant force exerted on the column by the pressure at the ends of the column. Equation (3a)

indicates that the gain of energy in the column results only from the pressure forces. The rate of increase of energy is equal to the power input, which is the work performed per unit time by pressure against the ends of the column.

For the development of the Rankine-Hugoniot conditions, assume that there is a discontinuity in the column. Assume that the discontinuity is at a point, $x = \Xi(t)$, and let u, P, ρ, and S be discontinious at this point. The discontinuity will move with a velocity $\frac{\partial \Xi}{\partial t}$, which will be denoted by U(t).

Upon examination of equations (1a-4a), it is seen that all of the integrals have the same form:

$$H = \int_{a_o(t)}^{a_1(t)} Y(x,t)\, dx \tag{5}$$

where the variable Y(x,t) is discontinious at the point, $x = \Xi$.

When the derivative of H is taken with respect to t, the following equation results.

$$\frac{dH}{dt} = \frac{d}{dt}\int_{a_o(t)}^{\Xi(t)} Y(x,t)\, dx + \frac{d}{dt}\int_{\Xi(t)}^{a_1(t)} Y(x,t)\, dx \tag{6}$$

The right side of equation (6) is evaluated by Courant (9) in

the following manner:

$$\frac{dH}{dt} = \int_{a_o(t)}^{a_1(t)} \frac{\partial Y(x,t)}{\partial t}\, dx + \left(\underset{(x \to \Xi)-}{\text{Lim}}\ Y(x,t)\right) \dot{\Xi}(t) - Y(a_o,t)\, u(a_o,t) + Y(a_1,t)\, u(a_1,t) - \left(\underset{(x \to \Xi)+}{\text{Lim}}\ Y(x,t)\right) \dot{\Xi}(t) \tag{7}$$

where

$$u(a_o,t) = \frac{\partial a_o(t)}{\partial t}$$

and

$$u(a_1,t) = \frac{\partial a_1(t)}{\partial t}$$

The notation $(x \to \Xi)-$ indicates that x approaches Ξ from the negative side of Ξ and $(x \to \Xi)+$ indicates that it approaches from the positive side.

Equation (7) holds independent of the length of the column, provided Ξ is an interior point. If the symbols Y_o and Y_1 are defined as:

$$Y_o = \underset{(x \to \Xi)-}{\text{Lim}}\ Y(x,t)$$

and

$$Y_1 = \underset{(x \to \Xi)+}{\text{Lim}}\ Y(x,t)$$

then in the limit, when the length of the column approaches zero, the integral

$$\int_{a_o(t)}^{a_1(t)} \frac{\partial Y(x,t)}{\partial t}\, dx$$

approaches zero, $Y(a_o,t) \to Y_o$, and $Y(a_1 t) \to Y_1$, so that equation (7) may be written:

$$\operatorname*{Lim}_{(a_1 \to u_o \to o)} \left(\frac{\partial H}{\partial t}\right) = Y_1 u_1 - Y_1 \dot{\Xi}(t) + Y_o \dot{\Xi}(t) - Y_o u_o \tag{8}$$

Using the notation, U, for the velocity of the shock front

v_i may be defined as $v_i = u_i - U$ $\qquad i = 0,1$

Thus,

$$\operatorname*{Lim}_{(a_1 \to a_o \to o)} \left(\frac{dH}{dt}\right) = Y_1 v_1 - Y_o v_o \tag{9}$$

Using equation (9) to evaluate equations (1a-4a) across a discontinuity, the following Rankine-Hugoniot conditions may be derived.

(1b) Conservation of Mass

$$\rho_1 v_1 - \rho_o v_o = 0$$

or

$$\rho_1 v_1 = \rho_o v_o = M \tag{10}$$

Here M is defined as the mass flux through the surface of discontinuity.

(2b) Conservation of Momentum

$$(\rho_1 u_1)\, v_1 - (\rho_o u_o)\, v_o = P_o - P_1$$

This equation can be rewritten in the form:

$$\rho_o v_o\, (v_o + U) + P_o = \rho_1 v_1\, (v_1 + U) + P_1$$

or

$$\rho_o v_o^{\,2} + P_o = \rho_1 v_1^{\,2} + P_1 \tag{11}$$

(3b) Conservation of Energy

$$\rho_1(\tfrac{1}{2}u_1^{\,2} + e_1)\, v_1 - \rho_o(\tfrac{1}{2}u_o^{\,2} + e_o)\, v_o = P_o u_o - P_1 u_1$$

or, in terms of M as defined above under (10)

$$M(\tfrac{1}{2}u_o^{\,2} + e_o) + u_o P_o = M(\tfrac{1}{2}u_1^{\,2} + e_1) + u_1 P_1$$

This equation may be converted to the form:

$$M(\tfrac{1}{2}v_o + e_o + P_o V_o) = M(\tfrac{1}{2}v_1^{\,2} + e_1 + P_1 V_1) \tag{12}$$

Where V is the specific volume.

(4b) Increase in Entropy

$$\rho_1 S_1 v_1 - \rho_o S_o v_o > 0 \tag{13}$$

For a shock surface at which $M > 0$, equation (3b) may be written:

$$\tfrac{1}{2}v_o^{\,2} + e_o + P_o V_o = \tfrac{1}{2}v_1^{\,2} + e_1 + P_1 V_1$$

or

$$\tfrac{1}{2}v_o^{\,2} + i_o = \tfrac{1}{2}v_1^{\,2} + i_1 \tag{14}$$

where i is the specific enthalpy which is defined by the relation:

$$i = e + PV$$

Using $\rho_o v_o = \rho_1 v_1 = M$ and $Mu_o + 1\,P_o = Mu_1 + P_1$

it is possible to write $Mv_o + P_o = Mv_1 + P_1$, since $u_i = v_i + U$

Thus,

$$P_1 - P_o = M(v_o - v_1) \tag{15}$$

Multiplying equation (15) through by $(V_o + V_1)$ produces,

$$(V_o + V_1)(P_1 - P_o) = (V_o + V_1)\,M\,(V_o - V_1) \tag{16}$$

Remembering that $M = \frac{v_1}{V_1} = \frac{v_o}{V_o}$, $(V_o + V_1)M$ may be written as, $(v_o + v_1)$

Thus equation (16) may be written

$$(V_o + V_1)(P_1 - P_o) = (v_o^2 - v_1^2)$$

From equation (14),

$$i_1 - i_o = \tfrac{1}{2}(v_o^2 - v_1^2)$$

so that,

$$(P_1 - P_o)\left(\frac{V_o + V_1}{2}\right) = i_1 - i_o \tag{17}$$

Equation (17) indicates that the increase in enthalpy across a shock wave is due to the pressure difference on the mean volume.

Since $i = e + PV$ equation (17) may be written,

$$(V_o - V_1)\left(\frac{P_1 + P_o}{2}\right) = e_1 - e_o \tag{18}$$

This equation indicates that when the material supporting the shock wave is compressed across the shock there is an increase in internal energy in the compressed material which equals the work done by the mean pressure in performing the compression.

Equation (18) is known as the Hugoniot relation.

The Hugoniot Relation

The Hugoniot Relation, equation (18) may be rewritten as,

$$H(P,V) = e(P,V) - e(P_o,V_o) + (V - V_o)\left(\frac{P_1 + P_o}{2}\right) \qquad (19)$$

where (P_o,V_o) is the pressure and specific volume ahead of the shock and (P,V) represents the pressure and volume behind the shock.

It is worthwhile to note that the Hugoniot Relation is not dependent upon the flow velocity or position of the shock. It is a relation dependent only upon the thermodynamic variables P, V, and e which characterize the media. Thus the relation is already in the form of an equation of state. It is different from a complete equation of state in that it relates the thermodynamic variables for only one condition. It relates the variables only at a point directly behind and another point directly in front of the shock where the pressures and specific volumes have their maximum and minimum values, respectively.

When the relation is written in the form $H(P,V) = 0$, it characterizes all values (P,V) behind the shock wave which satisfy the jump conditions across the shock with the values of

(P_o,V_o) which are given for the material ahead of the shock. When H is plotted in the (P,V) plane, the resulting graph is known as the Hugoniot curve. The Hugoniot curve plays an important role in the equation of state that is used in this thesis and more information concerning this curve will be discussed when the equation of state is considered in the next chapter.

CHAPTER III

EQUATION OF STATE

Bethe (4) has shown that the hydrodynamic equations governing fluid flow yield a solution for shock wave propagation if a complete equation of state exists and the equation of state satisfies three conditions set forth in his paper. These three conditions were discussed in Chapter II and it was observed that they were satisfied for all known materials that do not undergo a change of phase over the pressure range associated with the shock wave being propagated. As a consequence, the hydrodynamic equations for the propagation of a shock wave may be solved, provided a complete equation of state is obtained for aluminum.

Since the hydrodynamic equations are to be solved with a digital computer, it is not necessary for one equation of state to cover the complete pressure range associated with the shock. It is possible to combine several different equations, each valid over a specific range, to give a complete equation over the pressure range of interest.

The equation of state chosen for this work, the Mie-Gruneisen equation, is derived in detail in Appendix B. The form of this equation is,

$$P - P_h = \frac{\gamma}{V} (e - e_h) \qquad (1)$$

where P, V, and e are the pressure, specific volume, and the specific internal energy. The pressure, P_h, and the specific internal energy, e_h, are known functions of the specific volumes, as shown in Appendix C, over the range that the Hugoniot curve is known. The symbol, γ, in this equation should not be confused with the gamma of an ordinary gamma-law gas. In this case, γ is the Gruneisen ratio and chosen to be in such a form that it is a function of one variable, the specific volume. Thus a complete P, e, V equation of state exists for pressures as high as the Hugoniot curve is known.

It is proposed for this work that the Hugoniot be broken up into three different pressure regions. The first region will be taken from data published by Walsh, et.al., (10,11). This experimental Hugoniot covers the pressure range up to one megabar. The second region to be considered will be for pressures above 20 megabars. In this region, the Hugoniot will be constructed from published data of the Thomas-Fermi Statistical model of a plasma, which the material will approach at these high pressures. Since the available experimental Hugoniot extends to only one megabar and the Thomas-Fermi data is not considered valid under 20 megabars, it is necessary to interpolate between the values of the Hugoniot for the upper and lower regions.

EXPERIMENTAL HUGONIOT

The Hugoniot curve for 24ST aluminum has been experimentally measured up to 1 megabar by a method described in Appendix C. Rice, et.al., (11) analytically fit a cubic polynomial to their

experimental values which has the form,

$$P_h = A\mu + B\mu^2 + C\mu^3 \qquad (2)$$

where A, B, and C are constants determined by the shape of the curve and,

$$\mu = \left(\frac{V_o}{V} - 1\right)$$

V = specific volume

V_o = specific volume of the material in its unstressed state.

The Hugoniot in this form is a function of the specific volume and this permits the Mie-Gruneisen equation to fulfill the requirements of a complete P, e, V equation of state.

The Hugoniot from Thomas-Fermi Statistics

At the high pressure which results from a high velocity impact, the target material is believed to be momentarily converted to a plasma. The motion of the particles in this plasma can be described by Thomas-Fermi Statistics (12,13). This model involves reasonable assumptions which allow theoretical calculations of thermodynamic variables at high pressures. The assumptions that are necessary to permit theoretical calculation yield equations that are so complex that the only practical method of evaluating them is with a digital computer. These equations have been solved and the data obtained has been published and is available for use. (12,13)

Even though published data is available to reasonably low pressures, it is thought that the necessary assumptions limit the

validity of the data to pressures above 20 megabars. If the experimental Hugoniot is used for pressures up to 1 megabar and the Thomas-Fermi data is used to aid the construction of a Hugoniot for pressures above 20 megabars, there remains a region of uncertainty between 1 and 20 megabars in which the Hugoniot must be interpolated.

The curves plotted in figures (1) and (2) were prepared from the published data by Mr. B. A. Sodek. Figure (1) is a composite graph of the known experimental Hugoniot and the theoretically calculated thermodynamic variables at high pressures. In the higher pressure range, the lower bounding curve is the $0^{\circ}K$ isotherm. The network of curves in the higher pressure-range is composed of isotherms and constant entropy curves. Figure (2) is a plot of the same network of theoretical calculations over a larger pressure range.

There are several facts (14) which assist the construction of the Hugoniot above 20 megabars. First, it is known that across a strong shock the specific entropy increases. As a consequence, the Hugoniot curve must intersect the constant entropy curves as the pressure is increasing in order for the entropy to increase across the shock. A second known fact is that $\frac{dP}{dV} < 0$ along the Hugoniot. Third, the pressure along the Hugoniot varies from one atmosphere to a very high value while the specific volume varies from maximum value, V_o, to a minimum value, V_{min}. A fourth known fact is that a linear plot of P vs V for the Hugoniot is convex upward and any ray passing through any point on the Hugoniot

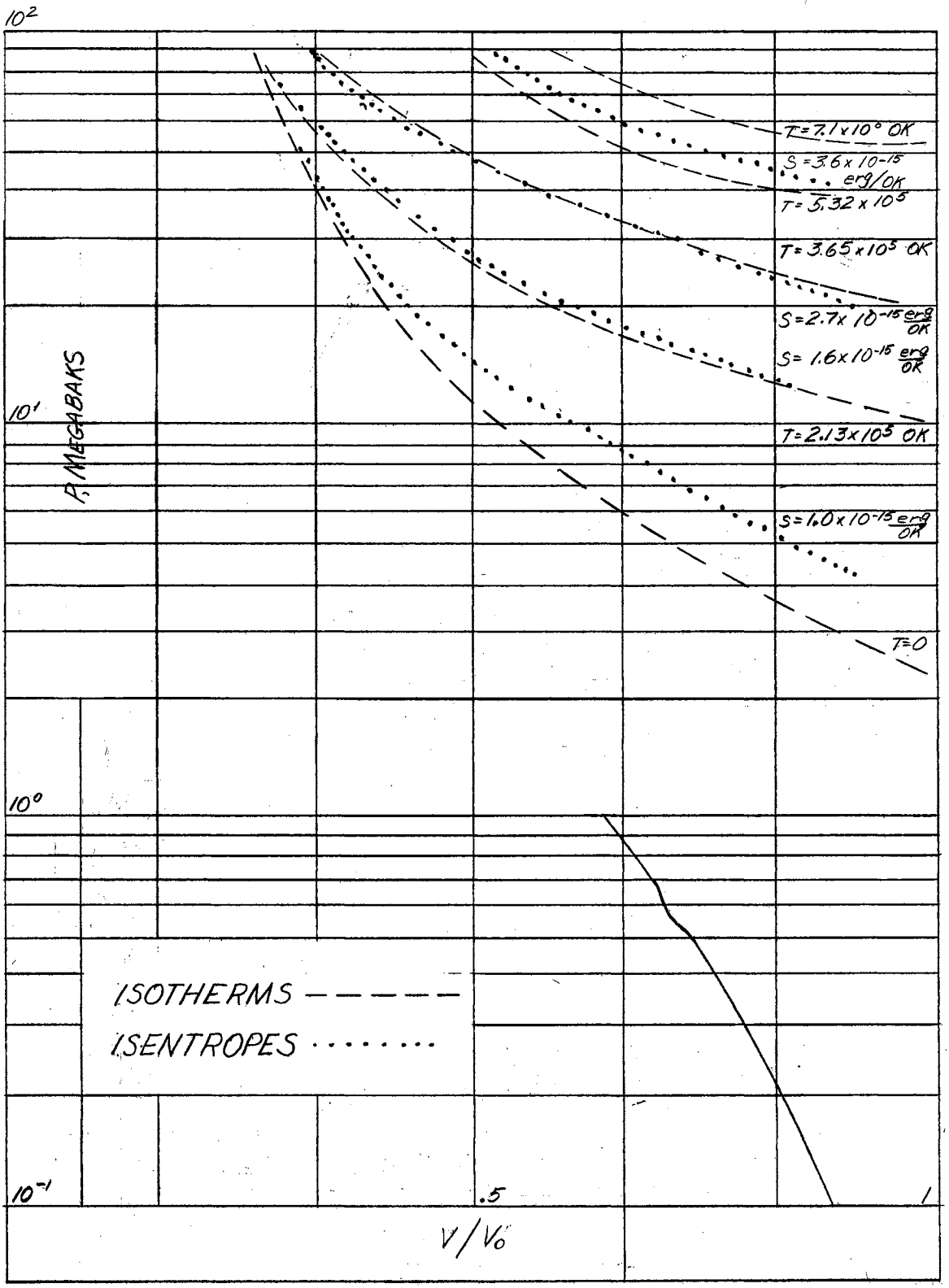

FIG. 1. EXPERIMENTAL HUGONIOT AND DATA FROM THE THOMAS - FERMI STATISTICS

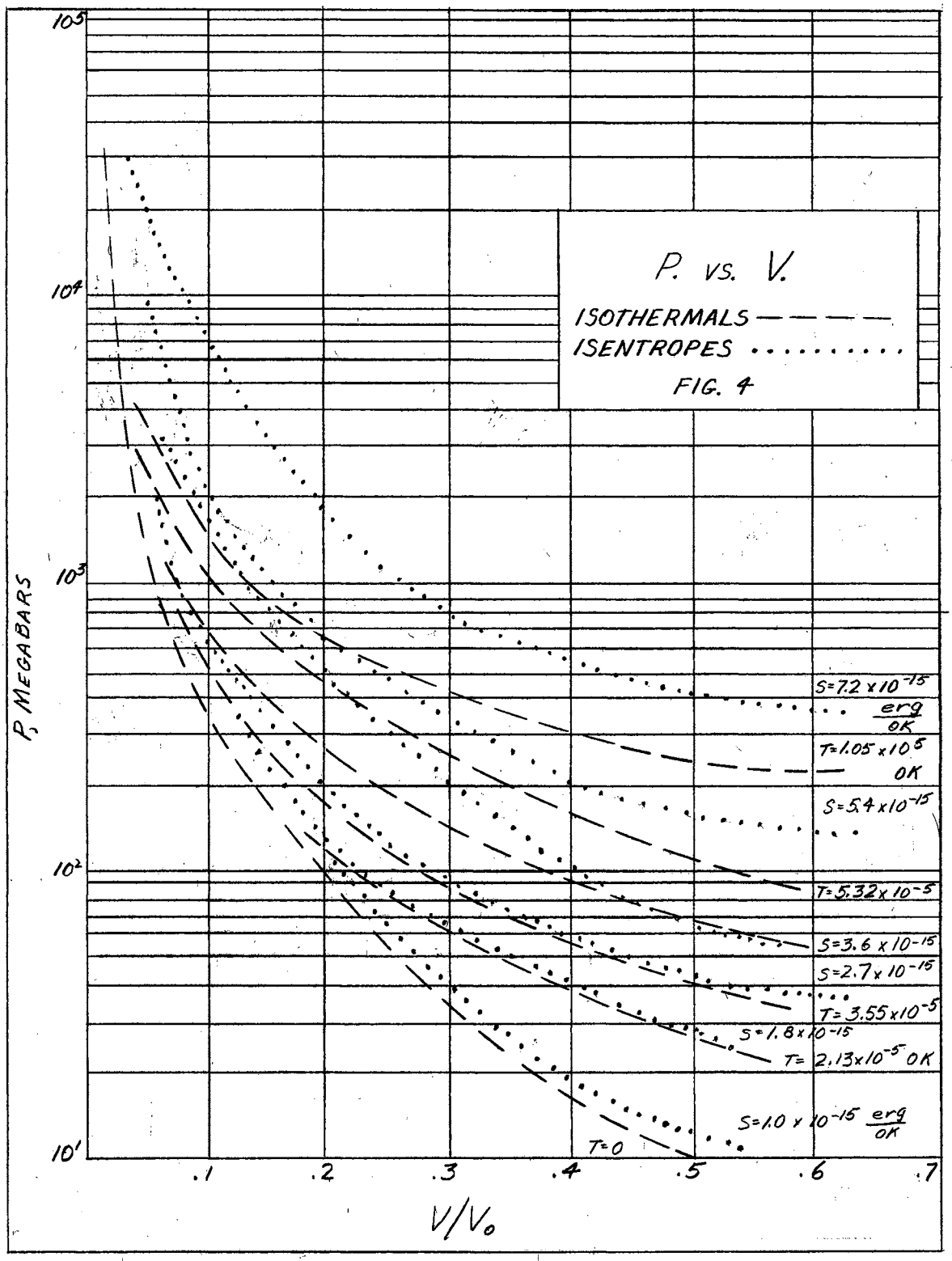

FIG. 2. THOMAS-FERMI STATISTICS FOR ALUMINUM

intersects the Hugoniot at one and only one other point, provided the ray intersects the V axis at a point $V \geq V_o$.

A linear plot of the Hugoniot curve that is used for P_h and V_h in the complete equation of state is presented in Figure 3. In this figure, the 0^oK isotherm is extrapolated from the 500 kilobar region to intersect the 0^oK isotherm from the Thomas-Fermi calculations at about 20 megabars. The Hugoniot plotted in this figure is a composite curve of the data of Rice et.al. (11), the Hugoniot constructed in the high pressure region, and the extrapolation between the two. The curves were analytically fit to the form,

$$P = A\mu + B\mu^2 + C\mu^3$$

where A, B, and C are constants and

$$\mu = \left(\frac{V_o}{V} - 1\right) = \left(\frac{\rho}{\rho_o} - 1\right)$$

The constants were evaluated to give the best fit of the data by the method of least mean square (15). In order to use the same analytical form for the complete pressure range, it was necessary to use three different sets of constants in three separate ranges. Table I contains the constants for both the Hugoniot and 0^oK isotherm and lists the specific volume ranges in which they are valid.

Although the Hugoniot constructed in Figure (1) is probably not absolutely correct, it does approximate a true Hugoniot

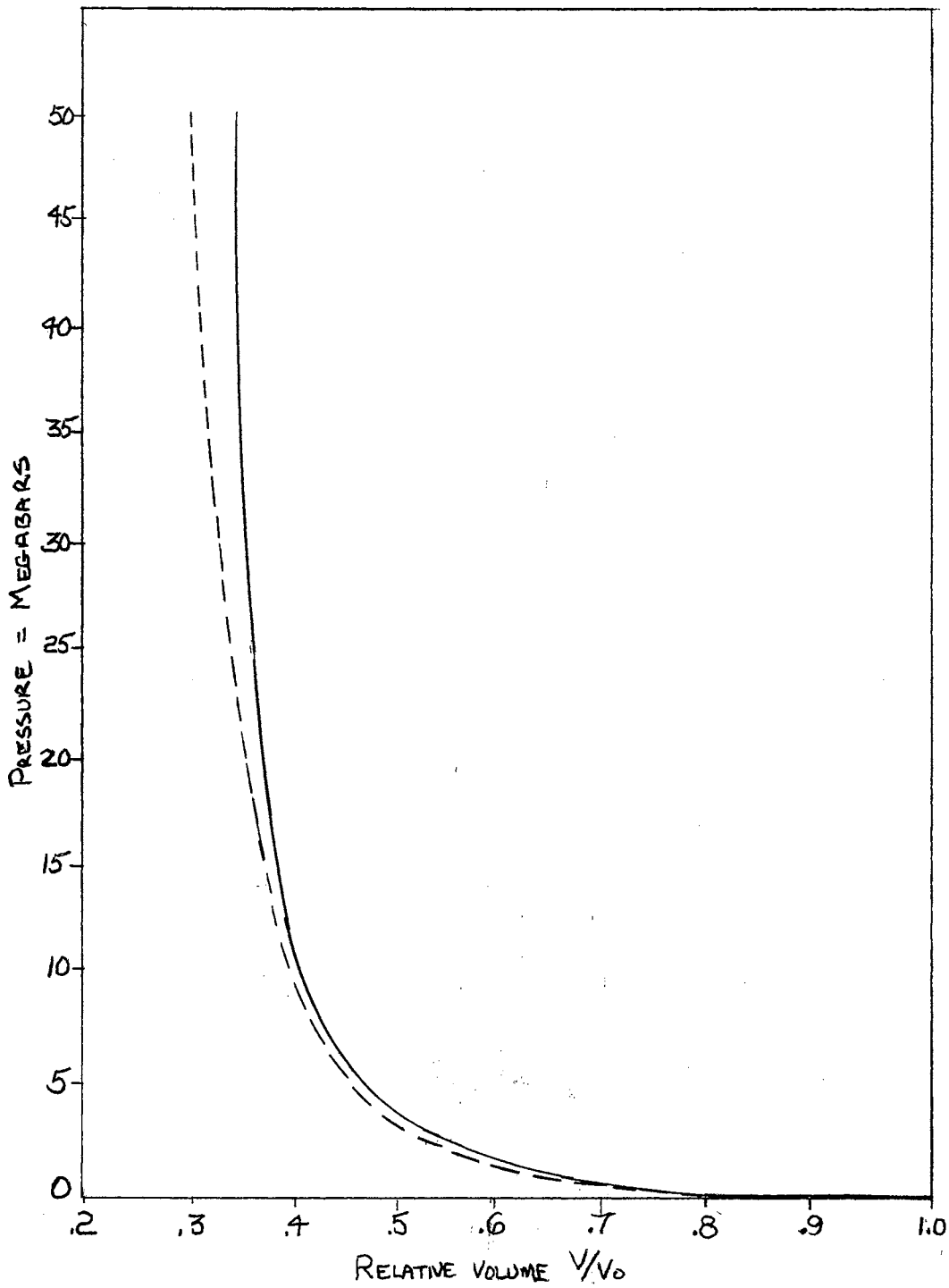

FIG. 3, COMPOSITE HUGONIOT AND ZERO DEGREE ISOTHERM FOR ALUMINUM

sufficiently well so the solution for the shock wave propagation is obtained with fair accuracy.

Computation of the Gruneisen Ratio

In order to have a complete P, e, V equation of state, it is necessary to know the value of the Gruneisen Ratio as a function of the specific volume over the complete pressure range. McQueen, et.al., assumed that the Gruneisen Ratio could be expressed in the form of the following series and evaluated the coefficients for the pressure range in which they were interested.

$$\gamma = \gamma_o + A\mu + B\mu^2 + C\mu^3 \tag{3}$$

Since the 0^oK isotherm and the Hugoniot are known as a function of the volume over the pressure range of interest, it is possible to compute γ from Equation (13) of Appendix B as a function of the volume

$$\gamma = \frac{V(P_h - P_k)}{\frac{1}{2}P_h(V_o - V) + e_o + \int_{V_o}^{V} P_k \, dV} \tag{4}$$

The Gruneisen ratio for this problem was computed from this relation by using the form of the 0^oK isotherm and the Hugoniot that was analytically fit to the curves in Figure (3). The resulting curve for γ was represented by a series of this form,

$$\gamma = \gamma_o + A\mu + B\mu^2 + C\mu^3$$

As for the equation of state, it was necessary to break the curve up into three different regions in order to obtain a more accurate representation of the variation for the range of specific volume considered. The constants obtained for γ in the three ranges for computation are given in Table II. The ranges correspond to the pressure ranges for the equation of state.

TABLE I

CONSTANTS FOR THE ZERO DEGREE ISOTHERM

$\frac{V}{V_o}$	A	B	C	Pressure (in megabars)
1.0 to .579	0.680	1.536	0.468	0 to 1.486
0.579 to .450	-1.574	5.116	-0.206	1.486 to 5.003
0.457 to .260	-8.7154	11.620	-0.620	5.003 to 52.000

CONSTANTS FOR THE HUGONIOT

$\frac{V}{V_o}$	A	B	C	Pressure (in megabars)
1.0 to .650	765.0	1659.0	428.0	0 to 1.000
.650 to .518	1150.1	-851.9	3998.0	1.000 to 3.570
.518 to .300	-2194.2	4034.7	2604.3	3.570 to 52.000

TABLE II

CONSTANTS FOR GRUNEISEN'S RATIO

$\frac{V}{V_o}$	γ_o	A	B	C	Pressure (in megabars)
1.0 to .650	2.130	-5.193	12.098	12.550	0 to 1.000
.650 to .518	2.000	-4.513	6.800	-3.780	1.000 to 3.570
.518 to .300	1.590	-1.355	.439	.0404	3.570 to 52.000

CHAPTER IV

APPLICATION OF THEORY

The Differential Equations of Fluid Dynamics

Fluids differ from solids under normal conditions by the property that the particles of the fluid have no resistance to shear. Compared to the tremendous forces that are initiated by micrometeoroid impact, the forces of a solid that resist shear may be regarded as insignificant. The yield strength of very good steel for instance, is on the order of 0.0068 megabars (16). This amounts to approximately 0.05% of the total impact force for the problem of micrometeoroid impact being considered. Since the shear forces are so insignificant for a problem of this type, the motion of material due to micrometeoroid impact on a solid target may be treated by the differential equations for the flow of a compressible fluid.

Courant (17) indicates that the system of differential equations that govern the flow of a compressible fluid must express the following physical laws:

a. The principle of conservation of mass

b. The conservation of momentum

c. The conservation of energy

d. The condition that changes of state are adiabatic except at the shock front.

The addition of an equation of state to these conditions completes the system of equations which are necessary to obtain a solution for fluid motion.

The partial differential equations that describe fluid motion are usually written in one of two forms, either Eulerian or Lagrangian. Although both of these forms are due to Euler, (18) German mathematicians designated one form Eulerian and the other Lagrangian. The Eulerian equations describe the variables at fixed points in space as time varies. Lagrangian equations describe the motion of individual particles or cells in the fluid and are most generally used for problems involving only one space variable such as problems of radial or slab symmetry. For problems of one space variable, the Lagrangian equations give more information than the Eulerian form, (19) since each bit of fluid is labeled with its original coordinate so that its original position may be determined at any time, t. It is also a property of Lagrangian equations that conservation of mass is automatic, even when the equations are converted to a finite difference form. This property enhances the accuracy of a numerical approximation to the true solution of fluid motion.

When problems involve more than one space variable, Eulerian equations are more often used. The accuracy of a Lagranian solution decreases for multidimensional systems as time increases unless a new space-time net is chosen. The choosing of a new net requires difficult and inaccurate interpolations. Therefore it is simpler to use the Eulerian form for this type of problem.

It is possible to derive the differential hydrodynamic equations

in either the Eulerian or Lagrangian system. For the present treatment the equations will first be examined in Eulerian coordiantes and later written in the Lagrangian form.

Eulerian Equations

Conservation of Mass:

The equation expressing the conservation of mass is the well known continuity equation often derived in standard mathematics texts (20).

The equation will not be derived here, but will be written in the form most often cited,

$$\frac{\partial \rho}{\partial t} + \nabla \cdot (\rho \vec{\Psi}) = 0$$

where

$$\nabla = \bar{i} \frac{\partial}{\partial X_1} + \bar{j} \frac{\partial}{\partial X_2} + \bar{k} \frac{\partial}{\partial X_3}$$

ρ is the density, and $\vec{\Psi}$ is the vector form of the fluid velocity $\bar{\Psi} = \bar{\Psi} \quad (X_1, X_2, X_3, t)$ in the orthoganal coordinate system, X_1, X_2, X_3.

For spherical flow, where the radial velocity is denoted as u and the radial Eulerian coordiante as R, the equation of continuity may be written as,

$$\frac{\partial \rho}{\partial t} + u\frac{\partial \rho}{\partial R} + \rho\left(\frac{\partial u}{\partial R} + \frac{2u}{R}\right) = 0 \qquad \text{(1a)}$$

Conservation of Momentum:

Conservation of Momentum is expressed by Newton's second law of motion which is that force equals mass times acceleration. This

law may be stated in equation form as,

$$\rho F_i - \frac{\partial P}{\partial X_i} = \rho \frac{d\Psi_i}{dt} \qquad (2a)$$

$$i = 1, 2, 3$$

where F_i represents body forces, $\frac{\partial P}{\partial X_i}$ is the pressure gradient and $\rho \frac{d\Psi_i}{dt}$ is the mass times the acceleration. The fluid velocity, Ψ_i, is a function of position and time:

$$\Psi_i = \Psi_i(X_1, X_2, X_3, t)$$

Therefore the derivative of Ψ_i with respect to t may be written as follows

$$\frac{d\Psi_i}{dt} = \frac{\partial \Psi_i}{\partial t} + \frac{\partial X_1}{\partial t} \cdot \frac{\partial \Psi_i}{\partial X_1} + \frac{\partial X_2}{\partial t} \cdot \frac{\partial \Psi_i}{\partial X_2} + \frac{\partial X_3}{\partial t} \cdot \frac{\partial \Psi_i}{\partial X_3}$$

or

$$\frac{d\Psi_i}{dt} = \frac{\partial \Psi_i}{\partial t} + \Psi_1 \frac{\partial \Psi_i}{\partial X_1} + \Psi_2 \frac{\partial \Psi_i}{\partial X_2} + \Psi_3 \frac{\partial \Psi_i}{\partial X_3}$$

and may be written in vector form as:

$$\frac{d\Psi_i}{dt} = \frac{\partial \Psi_i}{\partial t} + (\bar{\Psi} \cdot \nabla)\, \Psi_i$$

The assumption is made that body forces, such as gravity, are approximately equal to zero compared to the pressure gradient, $\frac{\partial P}{\partial X_i}$. By neglecting F_i, equation (2) may be rewritten,

$$\frac{1}{\rho} \frac{\partial P}{\partial X_i} + \frac{\partial \Psi_i}{\partial t} + (\bar{\Psi} \cdot \nabla)\, \Psi_i = 0 \qquad (2b)$$

For a spherical wave with radial velocity, u, the conservation of momentum is written,

$$\frac{\partial u}{\partial t} = u\frac{\partial u}{\partial R} + \frac{1}{\rho}\frac{\partial P}{\partial R} \tag{2c}$$

Conservation of Energy:

The flow after the impact is considered to be adiabatic except across the shock front. The change in entropy across the shock front is so important that the subject is considered in a separate section, although short section. All of the required thermodynamic variables in the complete equation of state must be evaluated and these are P, e and V, or ρ, where these symbols indicate the pressure, the energy, the volume and the density, respectively. Another relation between the variables in the problem may be obtained from the assumption that the gain of total energy by an increment of the fluid is only attributable to the work performed on the increment by the pressure (21). An additional assumption is made that viscous forces, body forces, heat conduction and energy sources are absent (22). Using these assumptions, the conservation of energy may be written in Eulerian, rectangular coordinates as follows:

$$\rho\frac{\partial e}{\partial t} + \rho\vec{\Psi}\cdot\nabla e + P\nabla\cdot\vec{\Psi} = 0 \tag{3a}$$

where $\vec{\Psi}$ is the vector velocity in rectangular coordinates. For spherical symmetry, the conservation of energy may be expressed in the form,

$$\rho\frac{\partial e}{\partial t} + \rho u\frac{\partial e}{\partial R} + P\left(\frac{2u}{R} + \frac{\partial u}{\partial R}\right) = 0 \tag{3b}$$

Further considerations of the change in entropy are considered in the next section.

Adiabatic Change of State:

The condition to insure an adiabatic change of state, except at points of discontinuity, is most often expressed by an equation that restricts the change in specific entropy:

$$\frac{\partial S}{\partial t} + \vec{V} \cdot \nabla S = 0 \qquad (4a)$$

This equation may be written for spherical motion with radial velocity, u, as follows,

$$\frac{\partial S}{\partial t} + u\frac{\partial S}{\partial R} = 0 \qquad (4b)$$

The adiabatic change of state must occur when a change in the specific entropy is restricted, by the use of equation (4). This equation has the physical significance that viscous forces and heat conduction do not occur in the flow at any point except across the shock front. At the shock front, a pseudo-viscosity term is introduced to make the solution possible with a digital computer.

The pseudo-viscosity term prevents the occurrence of uncontrolled oscillations at the shock front. These oscillations should be considered as vibrations of the discrete sections of materials that are defined by the difference equations. As the scale of these sections is decreased to approach infinitesimal dimensions, the pseudo-viscosity approaches more and more closely to reality.

With the set of equations (1-4), all of the necessary conditions

are expressed in Eulerian form, and written in terms of the thermodynamic variables P, e and V, or ρ. The Eulerian form for the equations was chosen for initial examination because it is easier to discuss and to recognize the origin of the terms than in the Lagrangian form of the equations. The equations will now be written in Lagrangian form to simplify computation of the numerical solutions.

Lagrangian Equations

For problems of one space variable such as the radial shock wave being considered, the differential equations for hydrodynamic flow are often used in the Lagrangian form. The reasons for selecting the Lagrangian coordinates for this problem have already been discussed. The equations express the same properties as the Eulerian equations and are written in a spherically symmetric form. Richtmyer (23) presents the spherical form of the equations as follows:

Conservation of Mass:

$$\frac{1}{\rho} = \frac{1}{\rho_o}\left(\frac{R(r,t)}{r}\right)^2 \frac{\partial R}{\partial r} \tag{5}$$

where r is the radial Lagrangian coordinate of a fixed coordinate system and R(r,t) is the radial Eulerian coordinate, ρ is a function of the Lagrangian coordinates and time, and ρ_o is the initial density.

Conservation of Momentum:

$$\frac{\partial u}{\partial t} = -\frac{1}{\rho}\left(\frac{R(r,t)}{r}\right)^2 \frac{\partial P}{\partial r} \tag{6}$$

where u is the radial fluid velocity and P is the static fluid pressure. Both u and P are functions of the Lagrangian coordiante and time, $u = u(r,t)$ and $P = P(r,t)$.

Conservation of Energy:

$$\frac{\partial e}{\partial t} = \frac{P}{\rho^2} \frac{\partial \rho}{\partial t} \tag{7}$$

where e, the internal energy per unit mass, is also a function of r and t.

The equation of state and the partial differential equation of the velocity are used to aid the three conservation equations in numerical solution of the problem.

Equation of State in the Mie-Gruneisen Form:

$$P - P_h = \gamma\rho(e - e_h) \tag{8}$$

where P and e are pressure and internal energy at any point in the P-e quadrant. P_h and e_h are the values of these quantities on the Hugoniot line. The quantity, γ, is the Gruneisen Ratio and changes slowly with the density.

Velocity:

$$u = \frac{\partial R(r,t)}{\partial t} \tag{9}$$

With the five equations (5-9), it is possible to solve for a numerical solution of the fluid motion at every point in the supporting media except the point where the shock exists.

The shock wave manifests itself in these equations as a point of discontinuity. J. von Neumann and R. D. Richtmyer, in 1950, proposed a method of introducing a fictitious, or pseudo-viscosity at this point of discontinuity which satisfies the condition that the entropy increases and permits a complete numerical solution of the fluid motion. Their method will be the topic of discussion in the next section.

The von Neumann-Richtmyer Method of Handling Shocks

Shock surfaces appear in the differential hydrodynamic equations as regions where the velocity, density, internal energy and other variables of the fluid are discontinuous. The Rankine-Hugoniot jump conditions were derived in Chapter II. These relations relate the conditions of the material on the two sides of the shock front and provide sufficient conditions to relate the differential equations on both sides of the shock (24). The process of applying boundary conditons to solve the propagation of a shock wave is known as a shock fitting. The problem was initially solved by an iterative trial and error calculation. Shock fitting is slow and certainly not satisfactory for more complicated problems.

J. von Neumann and R. D. Richtmyer, wishing to avoid the difficulties introduced by shock fitting, devised a method of automatically handling shock motion in the numerical solution of the differential equations (5). Their method treats shocks automatically whenever and wherever they arise. It is based on using a dissipative mechanism such as viscosity or heat conduction

which exist for real fluids (25). The introduction of a dissipative mechanism in the differential equations tends to smear the shock wave and change it from a discontinuity to a region where the variables are varying rapidly but continuously. Even though this method does away with the application of the boundary conditions, the Rankine-Hugoniot conditions still hold across the shock and the approximation of smearing out the shock can be made to represent actuality as accurately as desired by limiting the width of the shock.

von Neumann and Richtmyer proposed that the artificial dissipative mechanism be introduced in the form of a pseudo-viscosity term which can be added to the pressure. Upon the addition of this term, equations (6) and (7) can be written as follows,

$$\frac{\partial u}{\partial t} = -\frac{1}{\rho_o}\left(\frac{R(r,t)}{r}\right)^2 \cdot \frac{\partial (P + Q)}{\partial r} \qquad (10)$$

Conservation of Momentum

where Q is the dissipative term, and,

$$\frac{\partial e}{\partial t} = \frac{(P + Q)}{\rho^2} \cdot \frac{\partial \rho}{\partial t} \qquad (11)$$

Conservation of Energy

when equations (5), (8), (9), (10) and (11) are converted to a finite difference form, it is possible to solve them numerically in a stepwise manner with time by means of a digital computer. This method produces a solution in which shocks move with approximately the right velocity and has approximately the correct changes in

pressure, energy, density, and velocity across the shock boundary.

Selection of a Dissipative Mechanism

The dissipative term, Q, in the equations is artificially introduced to produce desired mathematical effects. For this reason, it is possible to use a Q term which is a function of any of the variables involved in the numerical calcualtion as long as it satisfies the following four requirements set forth by von Neumann and Richtmyer (5).

(1) The three conservation equations must have solutions without discontinuities.

(2) The thickness of the shock layers must be everywhere of the same order of magnitude as the interval length, Δr, used in the numerical computation, independent of the strength of the shock and of the condition of the material into which the shock is moving.

(3) The effect of the terms containing Q in the conservation of momentum and in the conservation of energy equations must be negligible outside of the shock layers.

(4) The Rankine-Hugoniot jump conditions must hold when all other dimensions characterizing the flow are large compared to the shock thickness.

The form of Q used in the problem solved in this thesis is patterned after the one recommended by Richtmyer (26), and is basically the same as the term used by Brode (27) in his solution of a spherical shock wave.

$$Q = -K_1^2 \rho\left(\frac{\partial u}{\partial r}\right) \cdot \left| \frac{\partial u}{\partial r} \right| \qquad (12)$$

where K_1 is a constant with length dimensions; $K_1 = a \Delta r$ and a is a constant.

It is known that the thickness of the shock zone is proportional to the coefficient of the dissipative mechanism (25) and therefore it is possible to control the width of the shock wave by choosing the value of K_1.

Dimensionless Differential Equations

For the computer solution of the Lagrangian differential equations, it is desirable to reduce the variables to dimensionless parameters to aid in numerical computations. Brode (27) devised a method which accomplishes this conversion and reduces the number of parameters in the equations by one. The pressure, p, density, ρ, and velocity, u, can be expressed in units of the initial pressure, P_o, initial density, ρ_o, and velocity, C_o. Brode chose to let the length variable be expressed in terms of a length ϵ which is a ratio of the total energy and ambient pressure, P_o.

$$\epsilon^3 = \frac{E_{total}}{P_o} \tag{13}$$

where E_{total} is the total energy involved in the shock wave and P_o is the pressure ahead of the shock wave.

For the problem solved in this thesis it is not necessary to restrict ϵ in the above manner and its value is arbitrarily chosen to scale the dimensions of the problem to a size convenient for machine solution.

The value of the Eulerian variable R(r,t) will be expressed as follows:

$$\lambda = \frac{R(r,t)}{\epsilon} \qquad \text{and} \qquad \lambda_o = \frac{r}{\epsilon} \tag{14}$$

where λ is the dimensionless Eulerian parameter at time = t, and λ_o is the dimensionless Eulerian parameter at time = 0. The dimensionless parameter for time, τ, is expressed as,

$$\tau = \frac{tc_o}{\epsilon} \tag{15}$$

where C_o is a constant velocity chosen to scale the problem for machine solution.

The dimensionless parameter representing the Lagrangian coordinate r can be expressed as,

$$x_d = \frac{1}{3}\left(\frac{r}{\epsilon}\right)^3 \tag{16}$$

This form is chosen to permit the Lagrangian coordiante to be eliminated from the numerical calculation of the solution.

Using the defined parameters, the dimensionless form of the necessary equations may be written,

$$\frac{1}{\rho} = \lambda^2 \frac{\partial \lambda}{\partial x_d} \tag{17}$$

Conservation of Mass

$$\frac{\partial u}{\partial \tau} = -\lambda^2 \frac{\partial (P + Q)}{\partial x_d} \tag{18}$$

Conservation of Momentum

$$u = \frac{\partial \lambda}{\partial \tau} \tag{19}$$

Velocity

and

$$Q = -a^2 \Delta x_d^2 \left(\frac{\partial u}{\partial x_d}\right) \cdot \left|\frac{\partial u}{\partial x_d}\right| \tag{20}$$

where Δx_d is the increment of x_d to be used in numerical compulation.

The partial of the energy with respect to time, $\frac{\partial e}{\partial \tau}$, can be taken for the equation of state and eliminated between the equation of state and the conservation of energy. This will permit solution of the flow equations without solving for the internal energy.

If this is done, the following equation results:

$$\frac{P + Q}{\rho^2} \frac{\partial \rho}{\partial \tau} = \frac{\partial \left(\frac{P-P_h}{\gamma \rho} + e_h\right)}{\partial \tau} \tag{21}$$

It is possible to combine the velocity equation and the conservation of mass equation in the following manner:

Take the partial derivative of u with respect to x_d from the velocity equation.

$$\frac{\partial u}{\partial x_d} = \frac{\partial^2 \lambda}{\partial x_d \partial \tau} \tag{22a}$$

Take the partial derivative of $\frac{1}{\rho \lambda^2}$ with respect to τ from the conservation of mass equation.

$$\frac{\partial \left(\frac{1}{\rho \lambda^2}\right)}{\partial \tau} = -\left[\frac{2\rho \frac{\partial \lambda}{\partial \tau} + \lambda^2 \frac{\partial \rho}{\partial \tau}}{\rho^2 \lambda^4}\right] = \frac{\partial^2 \lambda}{\partial x_d \partial \tau} \tag{22b}$$

Using these two equations, it is possible to eliminate

$$\frac{\partial^2 \lambda}{\partial x_d \partial \tau}$$

and solve for

$$\frac{\partial \rho}{\partial \tau}$$

such that,

$$\frac{\partial \rho}{\partial \tau} = -\rho\left[\frac{2u}{\lambda} + \frac{\partial u/\partial x_d}{\partial \lambda/\partial x_d}\right] \tag{23}$$

This is the form in which the conservation of mass will be used.

With the equations in the proper differential form, it is necessary to convert them to difference equations. The next section will deal with the method of differencing the equations and the form of the difference equations to permit a stepwise numerical solution.

Method of Finite Differences

If the hydrodynamic differential equations are to be solved numerically, it is necessary to convert them to finite difference equations. The accuracy of the solution is dependent upon the method used to difference the equations.

To indicate the manner in which equations are differenced, consider a function $f = f(x,t)$. The change in this function with

time can be computed as follows:

Let time increase by a small increment Δt. The change in the function is,

$$\Delta f(x,t) = f(x,t + \Delta t) - f(x,t) \tag{24}$$

This difference is defined as a forward difference. A backward difference is defined as,

$$\Delta f(x,t) = f(x,t) - f(x,t - \Delta t) \tag{25}$$

Although both forward and backward differences yield approximate solutions for the change in a function, they are not the most accurate finite differences that can be used. Wherever possible, central differences are used to represent the change in a function because the approximation to the true solution is more accurate. Forward and backward differences are most generally used at the boundaries of a problem where central differences will not give an answer. The central difference is defined as,

$$\delta_t f(x,t) = f(x,t + \tfrac{1}{2}) - f(x,t - \tfrac{1}{2}\Delta t) \tag{26}$$

where δ_t is the central difference operator and the difference is taken about the time, t.

Still considering the function f(x,t), let Δx and Δt be

increments of the variables x and t. A rectangular net, or grid, for the x and t plane is defined as the set of points $x = L\Delta x$ and $t = n\Delta t$

where $L = 1, 2, 3 \ldots\ldots L_{final}$

and $n = 1, 2, 3 \ldots\ldots\ldots n_{final}$

The function f(x,t) can be represented at any point in the net as,

$$f(L\Delta x, n\Delta t) = f_L^{n-\frac{1}{2}} \tag{27}$$

The value of the function at intermediate points in the net is written as,

$$f\left(\tfrac{1}{2}[L\Delta x + (L - 1)\Delta x], \tfrac{1}{2}[n\Delta t + (n - 1)\Delta t]\right) = f_{L-\frac{1}{2}}^{n-\frac{1}{2}} \tag{28}$$

It is possible, therefore, to denote the use of a central difference to replace a partial derivative of f(x,t) in an equation as follows,

$$\frac{\partial f(x,t)}{\partial t} = \frac{f_L^{n+\frac{1}{2}} - f_L^{n-\frac{1}{2}}}{\Delta t} \tag{29}$$

The increments in t and x must be small in order for the finite difference to approach the true value of the partial derivative. Thus when choosing Δx and Δt, one must choose between accuracy of the solution and feasibility of taking the time to solve the problem being considered with a very fine net.

With this brief introduction to finite differences the author will cite several references to methods of solving differential equations by finite differences. The equations

pertinate to the present problem will then be differenced. R. D. Richtmyer (19) gives a fairly complete discussion of solving initial value problems by difference methods. There are numerous other works of interest (28, 29, 30, 31).

Difference Equations

The difference equations given in this section are similar to those used by Brode (27) in his solution of a spherical blast wave, but differ from his exact equations in that his solution was for a Gamma-Law gas which utilized an ideal gas equation of state.

The differential equation of conservation of momentum, equation (18), can be a centrally differenced about the time point $n\Delta\tau$ and the space point $L = x_d$ as follows,

$$\frac{u_L^{n+\frac{1}{2}} - u_L^{n-\frac{1}{2}}}{\Delta\tau} = -\left(\lambda_L^n\right)^2 \left[\frac{P^n_{L+\frac{1}{2}} - P^n_{L-\frac{1}{2}} + Q^{n-\frac{1}{2}}_{L+\frac{1}{2}} - Q^{n-\frac{1}{2}}_{L-\frac{1}{2}}}{\Delta x_d}\right]$$

It may be noted that all variables except Q in the above equation are properly centered. Richtmyer (33) indicates that it is not worthwhile to rewrite this equation to center Q and, in fact, doing so might cause instabilities to arise in the numerical solution.

The velocity equation, (19), is differenced about the time point $(n+\frac{1}{2})\ \Delta\tau$ and the space point $L\Delta x$.

$$\frac{\lambda_L^{n+1} - \lambda_L^n}{\Delta\tau} = u_L^{n+\frac{1}{2}} \qquad (31)$$

The conservation mass equation, (23), is differenced about the time point $(n+\frac{1}{2})\,\Delta\tau$ and the space point $(L-\frac{1}{2})\,\Delta x$.

$$\frac{\rho_{L-\frac{1}{2}}^{n+1} - \rho_{L-\frac{1}{2}}^{n}}{\Delta\tau} = -\frac{\rho_{L-\frac{1}{2}}^{n+1} + \rho_{L-\frac{1}{2}}^{n}}{2}\left[\frac{2\left(u_{L}^{n+\frac{1}{2}} + u_{L-1}^{n+\frac{1}{2}}\right)}{\frac{\lambda_{L}^{n+1} + \lambda_{L}^{n}}{2} + \frac{\lambda_{L-1}^{n+1} + \lambda_{L-1}^{n}}{2}}\right.$$

$$\left. + \frac{\dfrac{u_{L}^{n+\frac{1}{2}} - u_{L-1}^{n+\frac{1}{2}}}{\Delta x_d}}{\dfrac{\frac{\lambda_{L}^{n+1} + \lambda_{L}^{n}}{2} - \frac{\lambda_{L-1}^{n+1} + \lambda_{L-1}^{n}}{2}}{\Delta x_d}}\right] \qquad (32)$$

This equation can be simplified to the form,

$$\rho_{L-\frac{1}{2}}^{n+1} - \rho_{L-\frac{1}{2}}^{n} = -\left(\rho_{L-\frac{1}{2}}^{n+1} + \rho_{L-\frac{1}{2}}^{n}\right) W \qquad (33a)$$

or

$$\rho_{L-\frac{1}{2}}^{n+1} = \rho_{L-\frac{1}{2}}^{n}\left(\frac{1 - W}{1 + W}\right) \qquad (33b)$$

where

$$W = \Delta\tau \left[\frac{2\left(u_L^{n+\frac{1}{2}} + u_L^{n-\frac{1}{2}}\right)}{\lambda_L^{n+1} + \lambda_L^{n} + \lambda_{L-1}^{n+1} + \lambda_{L-1}^{n}} + \frac{u_L^{n+\frac{1}{2}} - u_{L-1}^{n+\frac{1}{2}}}{\lambda_L^{n+1} + \lambda_L^{n} - \lambda_{L-1}^{n-1} - \lambda_{L-1}^{n}} \right]$$

The pseudo-viscosity equation, (21), used for this treatment may be differenced as follows,

$$Q_{L-\frac{1}{2}}^{n+\frac{1}{2}} = -a^2 (\Delta x_d)^2 \left(\frac{\rho_{L-\frac{1}{2}}^{n+1} + \rho_{L-\frac{1}{2}}^{n+1}}{2} \right) \left(\frac{u_L^{n+\frac{1}{2}} - u_{L-1}^{n+\frac{1}{2}}}{\Delta x_d} \right) \left| \frac{u_L^{n+\frac{1}{2}} - u_{L-1}^{n+\frac{1}{2}}}{\Delta x_d} \right| \quad (34)$$

The dissipative term written in this manner is unrestricted. That is, negative values of Q are allowed. It is suggested by some advocates of the pseudo-viscosity method (19, 27) that the value of Q should be set equal to zero outside of the shock zone in order to aid the numerical solution of the hydrodynamic variable where the supporting material is undergoing expansion. The form of Q in equation (34), however, is the form suggested by von Neumann and Richtmyer in their original work proposing the pseudo-viscosity method.

The method of eliminating the internal energy from the solution of the differential equation suggested previously

requires rigorous algebraic manipulation to convert the difference equation to a form that will permit a stepwise numerical solution of the hydrodynamic equations. To initiate this treatment, consider equation (21),

$$\frac{P + Q}{\rho^2} \frac{\partial \rho}{\partial \tau} = \frac{\partial \left[\frac{P - P_h}{\gamma \rho} + e_h \right]}{\partial \tau}$$

If the indicated differentiation is carried out, the following equation may be obtained,

$$\left(\frac{P + Q}{\rho^2} \right) \frac{\partial \rho}{\partial \tau} = \frac{Z \frac{\partial P}{\partial \tau} - Z \frac{\partial P_h}{\partial \tau} - (P - P_h) \frac{\partial Z}{\partial \tau}}{Z^2} + \frac{\partial e_h}{\partial \tau} \qquad (35)$$

where $Z = \gamma \rho$

This may be converted to the form,

$$Z^2 P \frac{\partial \rho}{\partial \tau} - Z \rho^2 \frac{\partial P}{\partial \tau} + \rho^2 P \frac{\partial Z}{\partial \tau} = \rho^2 P_h \frac{\partial Z}{\partial \tau} - Z^2 Q \frac{\partial \rho}{\partial \tau} - Z \rho^2 \frac{\partial P_h}{\partial \tau} + \rho^2 Z^2 \frac{\partial e_h}{\partial \tau} \qquad (36)$$

It is desirable to difference this equation about the time

point $n+\frac{1}{2}$ and the space point $L-\frac{1}{2}$.

$$\left[\frac{P^{n+1}_{L-\frac{1}{2}} + P^{n}_{L-\frac{1}{2}}}{2}\right] \cdot \left[\frac{Z^{n+1}_{L-\frac{1}{2}} + Z^{n}_{L-\frac{1}{2}}}{2}\right]^2 \cdot \left[\frac{\rho^{n+1}_{L-\frac{1}{2}} - \rho^{n}_{L-\frac{1}{2}}}{\Delta\tau}\right]$$

$$- \left[\frac{Z^{n+1}_{L-\frac{1}{2}} + Z^{n}_{L-\frac{1}{2}}}{2}\right] \cdot \left[\frac{\rho^{n+1}_{L-\frac{1}{2}} + \rho^{n}_{L-\frac{1}{2}}}{2}\right]^2 \cdot \left[\frac{P^{n+1}_{L-\frac{1}{2}} - P^{n}_{L-\frac{1}{2}}}{2}\right]$$

$$+ \left[\frac{\rho^{n+1}_{L-\frac{1}{2}} + \rho^{n}_{L-\frac{1}{2}}}{2}\right]^2 \cdot \left[\frac{P^{n+1}_{L-\frac{1}{2}} + P^{n}_{L-\frac{1}{2}}}{2}\right] \cdot \left[\frac{Z^{n+1}_{L-\frac{1}{2}} - Z^{n}_{L-\frac{1}{2}}}{\Delta\tau}\right]$$

$$= \left[\frac{\rho^{n+1}_{L-\frac{1}{2}} + \rho^{n}_{L-\frac{1}{2}}}{2}\right]^2 \cdot \left[\frac{P_h{}^{n+1}_{L-\frac{1}{2}} + P_h{}^{n}_{L-\frac{1}{2}}}{2}\right] \cdot \left[\frac{Z^{n+1}_{L-\frac{1}{2}} - Z^{n}_{L-\frac{1}{2}}}{\Delta\tau}\right]$$

$$- \left[\frac{Z^{n+1}_{L-\frac{1}{2}} + Z^{n}_{L-\frac{1}{2}}}{2}\right]^2 \cdot \left[Q^{n+1}_{L-\frac{1}{2}}\right] \cdot \left[\frac{\rho^{n+1}_{L-\frac{1}{2}} - \rho^{n}_{L-\frac{1}{2}}}{\Delta\tau}\right]$$

$$- \left[\frac{Z^{n+1}_{L-\frac{1}{2}} + Z^{n}_{L-\frac{1}{2}}}{2}\right] \cdot \left[\frac{\rho^{n+1}_{L-\frac{1}{2}} + \rho^{n}_{L-\frac{1}{2}}}{2}\right]^2 \cdot \left[\frac{P_h{}^{n+1}_{L-\frac{1}{2}} - P_h{}^{n}_{L-\frac{1}{2}}}{\Delta\tau}\right]$$

$$+ \left[\frac{\rho^{n+1}_{L-\frac{1}{2}} + \rho^{n}_{L-\frac{1}{2}}}{2}\right]^2 \cdot \left[\frac{Z^{n+1}_{L-\frac{1}{2}} + Z^{n}_{L-\frac{1}{2}}}{2}\right]^2 \cdot \left[\frac{e_h{}^{n+1}_{L-\frac{1}{2}} - e_h{}^{n}_{L-\frac{1}{2}}}{\Delta\tau}\right] \tag{37}$$

This rather involved equation is even further complicated when, for purposes of computation, the polynomial form of P_h, E_h, and γ from Chapter III are substituted. For Equation (37) to be of aid in the simultaneous solution of the system of hydrodynamic flow equations on the digital computer, it must be arranged in the form,

$$P^{n+1}_{L-\frac{1}{2}} = \frac{H(6)\left[2\left(H(4)\cdot H(1) - H(3)\cdot H(2) - H(1)\cdot P^{n}_{L-\frac{1}{2}}\right)\right]}{\left(H(1)+H(2)\right)^{2}\cdot\left(\rho^{n+1}_{L-\frac{1}{2}} - \rho^{n}_{L-\frac{1}{2}}\right) - 2H(2)\cdot H(6)}$$

$$+\frac{H(6)\left[\left(H(1)+H(2)\right)^{2}\cdot H(5) - \left(H(1)+H(2)\right)^{2}\cdot\left(\rho^{n+1}_{L-\frac{1}{2}} - \rho^{n}_{L-\frac{1}{2}}\right)\cdot\left(Q^{n+\frac{1}{2}}_{L-\frac{1}{2}} + P^{n}_{L-\frac{1}{2}}\right)\right]}{\left(H(1)+H(2)\right)^{2}\cdot\left(\rho^{n+1}_{L-\frac{1}{2}} - \rho^{n}_{L-\frac{1}{2}}\right) - 2H(2)\cdot H(6)} \qquad (38)$$

where

$$H(1) = Z^{n+1}_{L-\frac{1}{2}} = \rho^{n+1}_{L-\frac{1}{2}}\left[\gamma_o + A\mu^{n+1}_{L-\frac{1}{2}} + B\left(\mu^{n+1}_{L-\frac{1}{2}}\right)^2 + C\left(\mu^{n+1}_{L-\frac{1}{2}}\right)^3\right]$$

$$H(2) = Z^{n}_{L-\frac{1}{2}} = \rho^{n}_{L-\frac{1}{2}}\left[\gamma_o + A\mu^{n}_{L-\frac{1}{2}} + B\left(\mu^{n}_{L-\frac{1}{2}}\right)^2 + C\left(\mu^{n}_{L-\frac{1}{2}}\right)^3\right]$$

$$H(3) = P_{h}{}^{n+1}_{L-\frac{1}{2}} = A\mu^{n+1}_{L-\frac{1}{2}} + B\left(\mu^{n+1}_{L-\frac{1}{2}}\right)^2 + C\left(\mu^{n+1}_{L-\frac{1}{2}}\right)^3$$

$$H(4) = P_{h}{}^{n}_{L-\frac{1}{2}} = A\mu^{n}_{L-\frac{1}{2}} + B\left(\mu^{n}_{L-\frac{1}{2}}\right)^2 + C\left(\mu^{n}_{L-\frac{1}{2}}\right)^3$$

$$H(5) = \frac{1}{2}\left(e_{h}{}^{n+1}_{L-\frac{1}{2}} - e_{h}{}^{n}_{L-\frac{1}{2}}\right)$$

$$= \frac{1}{2}\left[\frac{A\left(\mu^{n+1}_{L-\frac{1}{2}}\right)^2 + B\left(\mu^{n+1}_{L-\frac{1}{2}}\right)^3 + C\left(\mu^{n+1}_{L-\frac{1}{2}}\right)^4}{\rho_o\left(\mu^{n+1}_{L-\frac{1}{2}} + 1\right)} - \frac{A\left(\mu^{n}_{L-\frac{1}{2}}\right)^2 + B\left(\mu^{n}_{L-\frac{1}{2}}\right)^3 + C\left(\mu^{n}_{L-\frac{1}{2}}\right)^4}{\rho_o\left(\mu^{n}_{L-\frac{1}{2}} + 1\right)}\right]$$

$$H(6) = \left(\rho^{n+1}_{L-\frac{1}{2}} + \rho^{n}_{L-\frac{1}{2}}\right)^2$$

where $\mu = (\rho - 1)$ in the dimensionless form.

To shorten the notation, the value of $P^{n+1}_{L-\frac{1}{2}}$ from Equation (38) will be denoted as,

$$P^{n+1}_{L-\frac{1}{2}} = f\left(P^{n}_{L-\frac{1}{2}},\ Q^{n+\frac{1}{2}}_{L-\frac{1}{2}},\ \rho^{n+1}_{L-\frac{1}{2}},\ \rho^{n}_{L-\frac{1}{2}}\right) \tag{39}$$

The differenced equations must now be arranged in a fashion that will permit a stepwise numerical solution. Equations (30), (31), (33), and (38) may be written in the following form:

$$\mu^{n+\frac{1}{2}}_{L} = \mu^{n-\frac{1}{2}}_{L} - \frac{\Delta\tau}{\Delta x_d}\left(\lambda^{n}_{L}\right)^{2}\left[P^{n}_{L+\frac{1}{2}} - P^{n}_{L-\frac{1}{2}} + Q^{n-\frac{1}{2}}_{L+\frac{1}{2}} - Q^{n-\frac{1}{2}}_{L-\frac{1}{2}}\right] \tag{40a}$$

$$\lambda^{n+1}_{L} = \lambda^{n}_{L} + \Delta\tau\mu^{n+1}_{L} \tag{40b}$$

$$\rho^{n+1}_{L-\frac{1}{2}} = \rho^{n}_{L-\frac{1}{2}}\left(\frac{1 - W}{1 + W}\right) \tag{40c}$$

$$Q^{n+\frac{1}{2}}_{L-\frac{1}{2}} = -a^{2}\left[\frac{\rho^{n+1}_{L-\frac{1}{2}} + \rho^{n}_{L-\frac{1}{2}}}{2}\right] \cdot \left(\mu^{n+\frac{1}{2}}_{L} - \mu^{n+\frac{1}{2}}_{L-1}\right) \cdot \left|\mu^{n+\frac{1}{2}}_{L} - \mu^{n+\frac{1}{2}}_{L-1}\right| \tag{40c}$$

$$P^{n+1}_{L-\frac{1}{2}} = f\left(P^{n+1}_{L-\frac{1}{2}},\ Q^{n+\frac{1}{2}}_{L-\frac{1}{2}},\ \rho^{n+1}_{L-\frac{1}{2}},\ \rho^{n}_{L-\frac{1}{2}}\right) \tag{40e}$$

If boundary and initial values of all the variables are known before and including time $t = n\Delta\tau$, the above set of equations when solved in the order that they appear, will permit a stepwise solution for the flow velocity, density, and pressure.

For actual machine computation the difference equations must be written in a language which can be punched on IBM cards and accepted by the IBM 650 digital computer. This conversion, along with the machine logic to solve the equations, will be considered in the next chapter.

CHAPTER V

DEVELOPMENT OF COMPUTER PROGRAM

The IBM 650, digital computer for solving the problem in this thesis is very limited in storage capacity. The computer memory consists of 2000 words of drum storage and 60 words of core (immediate access) storage. This small memory seriously limits the size and type of shock-problem that can be solved. The problem for the propagation of a spherical shock may be solved provided the computer program is written in the shortest possible manner. The short program will leave sufficient storage in the computer for a space-time net that is large enough to permit a numerical approximation of the proposed problem.

The program will be written in 650 FORTRAN (an automatic coding system for the IBM 650 which allows the user to write programs for the 650 without having a working knowledge of the computer). Use of the FORTRAN system consists of the following steps:

1. The logic and equations are written in FORTRAN (FORmula TRANslator).

2. The FORTRAN statements are processed by a 650 program called the FORTRAN compiler, or FORTRAN phase I, which accepts FORTRAN statements and compiles 650 instructions in SOAP II (Symbolic Optimal Assembly Program) language.

3. The SOAP II program is next processed by an

assembler program called FORTRAN Phase II, which is a modified version of a SOAP II assembler, that produces an optimized machine language program (Object Deck) from the symbolic instructions.

The machine language program produced by the FORTRAN, Phase II compiler is the final result of the compiling process. The Object Deck contains FORTRAN subroutines (special programs contained in the FORTRAN compiler) and the original FORTRAN program in a format that is acceptable to the computer for data processing.

Development of Machine Logic

In order that the difference equations may be solved by the 650, a logic must be developed which will permit the computer to accept the equations and solve them in a logical order. This logic can best be presented in the form of a flow diagram, Figure (4).

The solution of the set of simultaneous difference equations as they appear in Equations 40_a — 40_e in Chapter IV requires that each of the variables, u , ρ , λ , Q, and P, be contained in the 650 memory at the same time for each space net point at two different time points, say $n\,\Delta\tau$ and $(n+1)\,\Delta\tau$. With this information in the computer memory, it is possible to solve for the value of each of the variables for each net point at the time $(n+1)\Delta\tau$ from the initial value of the variable at the time $n\Delta\tau$.

The computations are carried out in the indicated order, Equation 40_a through 40_e. After the computation, the flow diagram shows that the new values for the variables at the time $(n+1)\,\Delta\tau$ replace the initial values so another set of variables may be

computed at the next step in time.

The variables are computed at every net point except the first by the difference equations. The value of the variables at the first net point must be stipulated by boundary conditions which will be discussed in Chapter VI.

Since computer storage is limited, it is impossible to place a sufficiently large net in the 650 storage to permit an initial shock profile to propagate through the net until the solution is obtained. The shock quickly fills the available net; therefore, it is necessary to devise a method to increase the size of the net, periodically, in order to follow the shock as it propagates through the material.

The method devised to keep up with increase in size of the problem is to permit the shock to move from the center to the end of the net and then to double the size of the space increments. This returns the shock to about the center of the available net spaces. The principle reason for choosing this particular method is that it permits the time increment to be increased without adding instabilities to the solution. This decreases the computer time that is necessary to obtain a final solution.

FORTRAN Equations

Once the logic is determined, it is necessary to convert the logic and the equations to FORTRAN statements. The logic steps are indicated in Figure (4) and expressed in FORTRAN language in Figure (5).

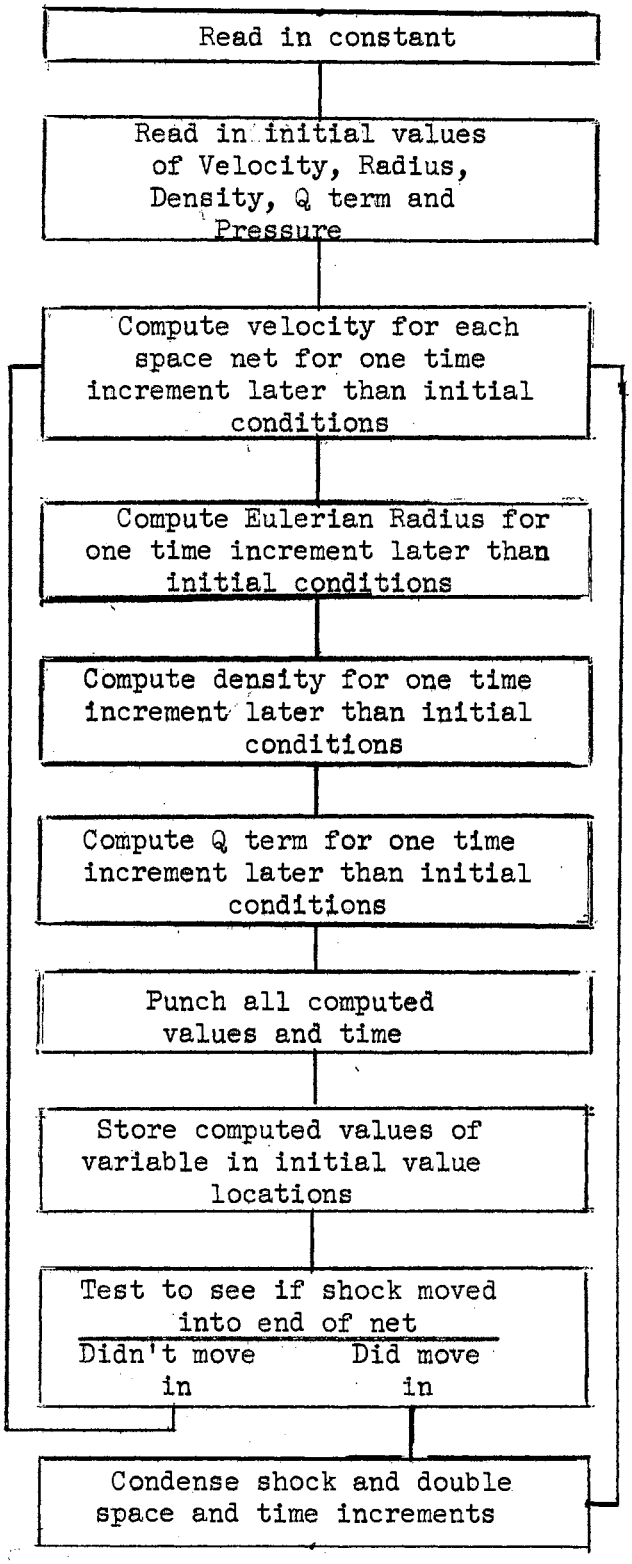

Figure 4 FLOW DIAGRAM

```
      GO TO 41
   39 0 N=9
      GO TO 41
   41 0 DO 42 I=1,3
   42 0 C(I)=C(I+N)
      DO 57 I=2,4
   57 0 B(I)=B(I+N)
      IF(N-6) 26,27,28
   26 0 B(1)=B(14)
      GO TO 29
   27 0 B(1)=B(15)
      GO TO 29
   28 0 B(1)=B(16)
   29 0 COUNT=COUNT+1.0
      IF(COUNT-2.0) 44,46,43
   43 0 STOP1
   44 0 GO TO 55
   55 0 H(3)=C(1)*T(2)+C(2)*(T(2)*T(2)
   55 1 )+C(3)*(T(2)*T(2)*T(2))
   45 0 H(1)=CD(L)*(B(1)+(B(2)*T(2))+(
   45 1 B(3)*(T(2)*T(2)))+(B(4)*(T(2)*
   45 2 T(2)*T(2))))
      IF(D(L)-DONE) 36,36,47
   47 0 IF(D(L)-DTWO) 38,38,39
   46 0 GO TO 60
   60 0 H(4)=C(1)*T(1)+C(2)*(T(1)*T(1)
   60 1 )+C(3)*(T(1)*T(1)*T(1))
   50 0 H(2)=D(L)*(B(1)+(B(2)*T(1))+(B
   50 1 (3)*(T(1)*T(1)))+(B(4)*(T(1)*T
   50 2 (1)*T(1))))
   65 0 H(5)=T(2)*H(3)/((4.0*DZERO)*(C
   65 1 D(L)))-(T(1)*H(4))/((4.0*DZERO
   65 2 )*(D(L)))
   70 0 H(6)=(CD(L)+D(L))*(CD(L)+D(L))
   75 0 Y(1)=H(6)*(2.0*((H(4)*H(1))-(H
   75 1 (3)*H(2))+(H(1)*P(L)))-((H(1)+
   75 2 H(2))*(H(1)+H(2))*H(5)))
   80 0 Y(2)=(H(1)+H(2))*(H(1)+H(2))*(
   80 1 CD(L)-D(L))-(2.0*(H(2)*H(6)))
   85 0 CP(L)=(Y(1)-(H(1)+H(2))*(H(1)+
   85 1 H(2))*((CD(L)-D(L))*2.0*CQ(L))
   85 2 )/Y(2)
      CQ(1)=0.0
      CD(1)=DX
      CP(1)=DT
      DO 90 I=1,J
   90 0 PUNCH1,CU(I),CR(I),CD(I),CQ(I)
   90 1 ,CP(I),I
      DO 95 I=1,J
      U(I)=CU(I)
      R(I)=CR(I)
```

```
    1 0 DIMENSION A(2),B(16),C(12),H(6
    1 1 ),Y(2),T(2)
    2 0 DIMENSION CU(65),CR(65),CD(65)
    2 1 ,CQ(65),CP(65),U(65),R(65),D(6
    2 2 5),Q(65),P(65)
      READ1,DX,DT,LFINL,DONE,DTWO
      DO 31=1,2
    3 0 READ2,A(I)
      DO 4 I=1,16
    4 0 READ3,B(I)
      DO 5 I=4,12
    5 0 READ4,C(I)
      J=LFINL
      DO 6 I=1,J
    6 0 READ5,U(I),R(I),D(I),Q(I),P(I)
      READ6,THRU,DZERO,M,ERROR
      TIME=0.0
      NET=0
      K=LFINL-1
    9 0 DO 10 L=2,K
   10 0 CU(L)=U(L)-((A(1)*DT*R(L)*R(L)
   10 1 *(P(L+1)-P(L)+Q(L+1)-Q(L)))/DX
   10 2 )
      CU(1)=0.0
      CU(J)=0.0
      DO 15 L=1,J
   15 0 CR(L)=R(L)+DT*CU(L)
      DO 25 L=2,J
   20 0 W=DT*(2.0*((CU(L)+CU(L-1))/(CR
   20 1 (L)+R(L)+CR(L-1)+R(L-1)))+((CU
   20 2 (L)-CU(L-1))/(CR(L)+R(L)-CR(L-
   20 3 1)-R(L-1))))
   25 0 CD(L)=D(L)*(1.0-W)/(1.0+W)
      DO 33 L=2,J
 1006 0 IF((CU(L)-CU(L-1))-1.0E22)31,
 1006 1 31,30
   30 0 CQ(L)=A(2)*((CD(L)+D(L))/2.0)*
   30 1 (CU(L)-CU(L-1))*(ABSF(CU(L)-CU
   30 2 (L-1)))
      GO TO 33
   31 0 CQ(L)=0.0
   33 0 CONTINUE
      DO 85 L=2,J
   35 0 T(2)=CD(L)-1.0
   40 0 T(1)=D(L)-1.0
      COUNT=0.0
      IF(CD(L)-DONE) 36,36,37
   36 0 N=3
      GO TO 41
   37 0 IF(CD(L)-DTWO) 38,38,39
   38 0 N=6
```

```
      D(I)=CD(I)
      Q(I)=CQ(I)
   95 0 P(I)=CP(I)
      TIME=TIME+1.0
      IF(TIME-THRU) 100,130,130
  100 0 IF(CD(M)-D(M)) 115,115,105
  105 0 DO 96 I=2,30
      U(I)=(U(2*I-1)+U(2*I-2))/2.0
      P(I)=(P(2*I-1)+P(2*I-2))/2.0
      Q(I)=(Q(2*I-1)+Q(2*I-2))/2.0
   96 0 D(I)=(D(2*I-1)*D(2*I-2))*2.0/
   96 1 (D(2*I-1)+D(2*I-2))
      DO 97 I=1,5
      U(I+30)=U(I+59)
      D(I+30)=D(I+59)
      Q(I+30)=Q(I+59)
   97 0 P(I+30)=P(I+59)
      DO 98 I=1,30
      U(I+35)=0.0
      D(I+35)=1.0
      Q(I+35)=0.0
   98 0 P(I+35)=0.0
      R1=R(1)
      DO 114 I=2,65
   99 0 CUBE=(R1*R1*R1+DX/D(I))
      ROOT=(CUBE/3.0)+.33333333
  111 0 R(I)=((CUBE/(ROOT*ROOT))+2.0*
  111 1 ROOT)/3.0
  112 0 IF(ABSF(ROOT-R(J))-ERROR) 114,
  112 1 114,113
  113 0 ROOT=R(I)
      GO TO 111
  114 0 R1=R(I)
      DX=2.0*DX
      DT=2.0*DT
      U(1)=0.0
      CP(1)=DT
      CD(1)=DX
      NET=NET+1
      DO 1000 I=1,65
 1000 0 PUNCH3,U(I),R(I),D(I),Q(I),
 1000 1 P(I)
  115 0 PUNCH2,TIME,NET
      GO TO 9
  130 0 STOP 2
      END
```

Fig. 5 FORTRAN PROGRAM

Although the FORTRAN system gave a complete SOAP II program, the size of the resulting program was too large for the available memory in the IBM 650 computer. Alterations in the SOAP program were made which reduced the information necessary to be stored in the memory. By changing the program in this manner, the SOAP program was sufficiently reduced so a net of 65 space points was available for two different instants in time for each of the five variables. It was found more convenient to make all minor changes in the overall program in the SOAP deck.

CHAPTER VI

INITIAL VALUES, BOUNDARY CONDITIONS, AND SOLUTIONS

The set of difference equations, 40a through 40e, given in Chapter IV have sufficient versatility to yield an exact solution of shock wave propagation for any arbitrary set of initial values and boundary conditions. If the exact mechanisms of micrometeoroid impact were known, the propagation of the associated shock wave could be readily solved. This is not the case; and consequently, initial values must be derived and boundary conditions assumed that will give an acceptable approximation to the true problem.

Initial Values

Initial values were chosen for the present treatment of micrometeoroid impact with two criteria in mind. First, initial conditions must be chosen so the problem to be solved will remain sufficiently simple for solution on the available IBM 650 digital computer. The second criteria, certainly no less important than the first, is that the chosen initial conditions must be an acceptable approximation of actual conditions that exist during micrometeoroid impact.

The model of impact chosen for the present problem is illustrated in Figure (6). It is assumed that a nickel-iron (density equal 8 gm/cm^3) micrometeoroid traveling with a velocity

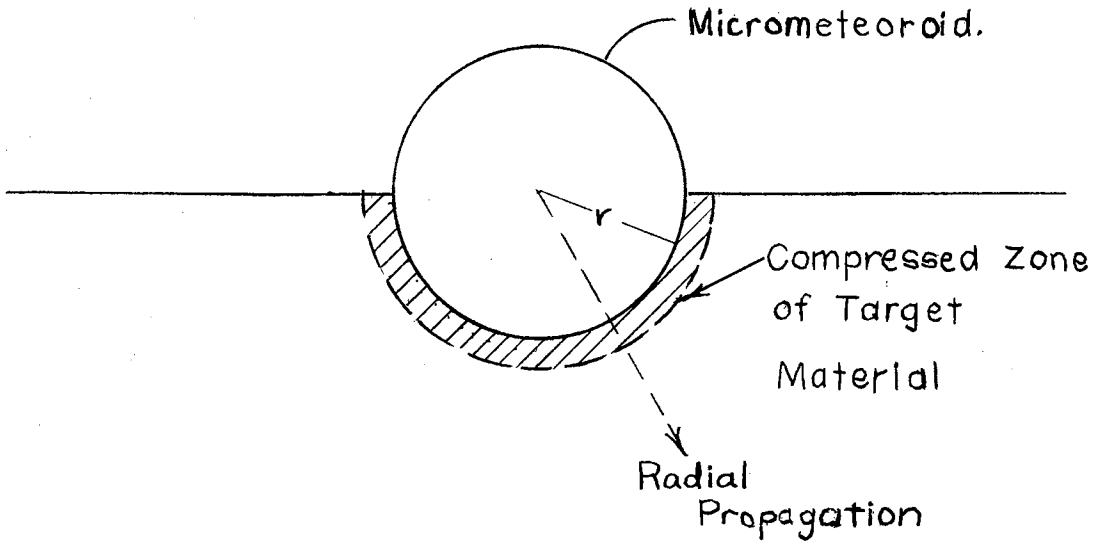

A. Assumed Initial Boundary Condition

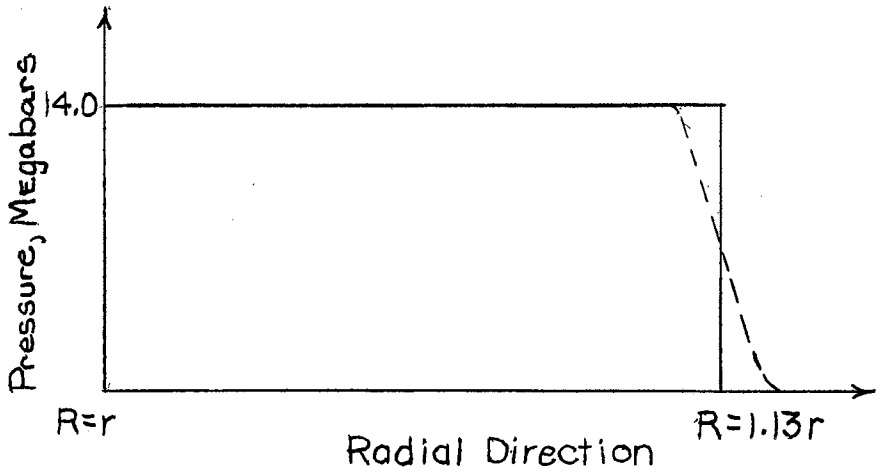

B. Assumed Step Shock Wave

Fig. 6. Assumptions for Impact of a Sphere.

of 36 kilometers per second impacts on a semi-infinite aluminum (density equal 2.70 gm/cm^3) target. The simplifying assumption is made that the spherical micrometeoroid is incompressible and enters the target by compressing a hemispherical shell of the target material ahead of it. This is illustrated in Figure (6a). A further simplifying assumption is that the pressure, density, and material velocity are constant in the compressed region at the instant illustrated. The pressure at the front of the compressed region drops sharply but not instantly. This is indicated in Figure (6b). The machine solution starts at the instant when the micrometeoroid has penetrated one-half of its diameter (3.1×10^{-4} cm) into the target.

These assumptions, combined with Rankine-Hugoniot conditions across the shock, and equations expressing conservation of momentum and energy between the micrometeoroid and target, allow calculations of the values of pressure, density, material velocity and dimensions of the compressed zone. An iterative method derived by Mr. J. G. Ables for making these calculations is given in Appendix D. The values for the material in the compressed zone of the target were determined by these calculations for impact by the micrometeoroid at 36 Km/second and are:

Pressure	14.1 Megabars
Velocity	17 Km/second
Density	6.7 gm/cm^3
Shock Radius	3.5×10^{-4} cm

The initial values for the problem are not the conditions that

truly exist for micrometeoroid impact. They are believed to approximate the true conditions sufficiently to indicate the order of magnitude of the true solution. This approximation is required to postulate conditions for more complex and more correct models of the impact.

Boundary Conditions

Boundary conditions for the problem of micrometeoroid impact must be in the form of one of the variables P, or u, at the micrometeoroid interface. To solve the set of equations 40a through 40e in the order indicated, the flow velocity, u, of the interface must be specified for any time, t. For actual micrometeoroid impact, the interface velocity will vary with time, decreasing as time increases. The boundary condition chosen for this order of magnitude problem is that the interface velocity equals zero after the instant that is illustrated in Figure (6a). This assumption is made for two reasons. First, it is necessary to choose a simple condition that permits the problem to be solved on the IBM 650. Second, this first approximation solution assumes no energy is transmitted to the target material by the micrometeoroid after time zero for the machine solution. The assumption of a rigid wall with zero velocity meets these requirements.

Parameters Chosen for Solution

The dimensionless parameters for this problem were chosen to give a convenient scaling for machine computations. Values of

P_o, ρ_o, and ϵ were arbitrarily chosen to scale the initial values of pressure, density, flow velocity, time and Eulerian radius to the number range 1 to 10^4. This range, being well centered in the 10^{-50} to 10^{50} range for the IBM 650, permits the problem to be solved without causing the machine to "overflow" (exceed the possible number range of the computer).

The values selected are,

$\epsilon = 5.49 \times 10^{-5}$ cm

$P_o = 1000$ Kilobar

$\rho_o = 2.7$ gm/cm^3

$C_o = 3.2 \times 10^4$ cm/sec

From these values it is possible to compute the actual time increment, Δt, from the dimensional increment $\Delta \tau$ as,

$$\Delta t = \frac{\epsilon \Delta \tau}{C_o}$$

The choice of values for increments of $\Delta \tau$, and Δx_d must be made from stability consideration.

Stability Conditions

The stability of the solution obtained by machine computation is dependent upon the net velocity and the size of the constant, a^2, used in the dissapative term. The net velocity must meet the Courant-Friedrichs-Lewy condition (34) that:

$$\frac{\Delta r}{\Delta t} \leq \text{the velocity of sound in the media.}$$

Brode (27) shows that this condition reduces to

$$\Delta \tau \leq \frac{\Delta x_d}{\lambda^2 (P\rho)^{\frac{1}{2}}_{max}} \qquad (1)$$

for the dimensionless equation.

To keep the solution stable for this particular problem, it was found necessary to keep $\Delta\tau$ below one-half of the value that is indicated by the Courant conditon.

The constant a^2 was obtained experimentally on the computer by trying several values in the problem. It was found that the solution would remain stable and the shock front would cover only 2 or 3 space nets if the value $a^2 = 2$ was used. Larger values caused the shock to spread out too much and smaller value caused instabilities to arise.

The Solutions

Shock wave pressure profiles are presented in Figures (7), (8), (9), and (10). The pressure is presented as a function of the radial distance from the point of impact and the scale in the figures is changed as time increases to allow a clearer presentation of the data. The initial shock pressure of 14.1 megabars drops to 1.7 megabars in $3\text{x}10^{-10}$ seconds and finally to below 0.5 megabars at time $9.2\text{x}10^{-10}$ seconds after time zero. The machine solution was carried to the time that the shock pressure was just under 0.5 megabars.

The flow velocities corresponding to the pressure profiles are presented in Figures (11), (12), (13), and (14). It is noted in Figure (12) that the velocity of the material in the immediate vicinity of the micrometeoroid, target interface is negative, indicating that the material is flowing back toward the micro-

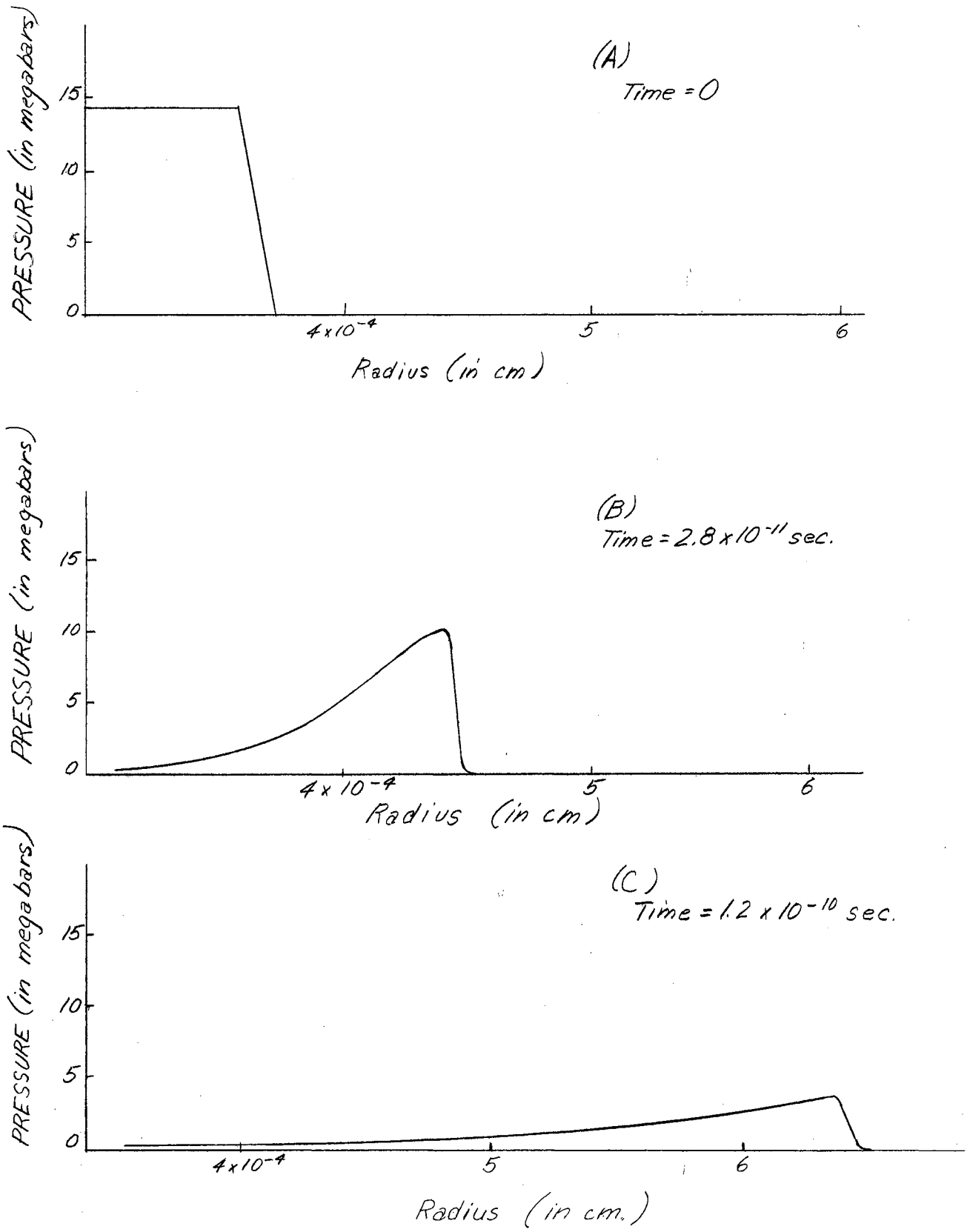

FIG. 7. PRESSURE PROFILES AT $T=0$, 2.8×10^{-11}, and 1.2×10^{-10} SECONDS

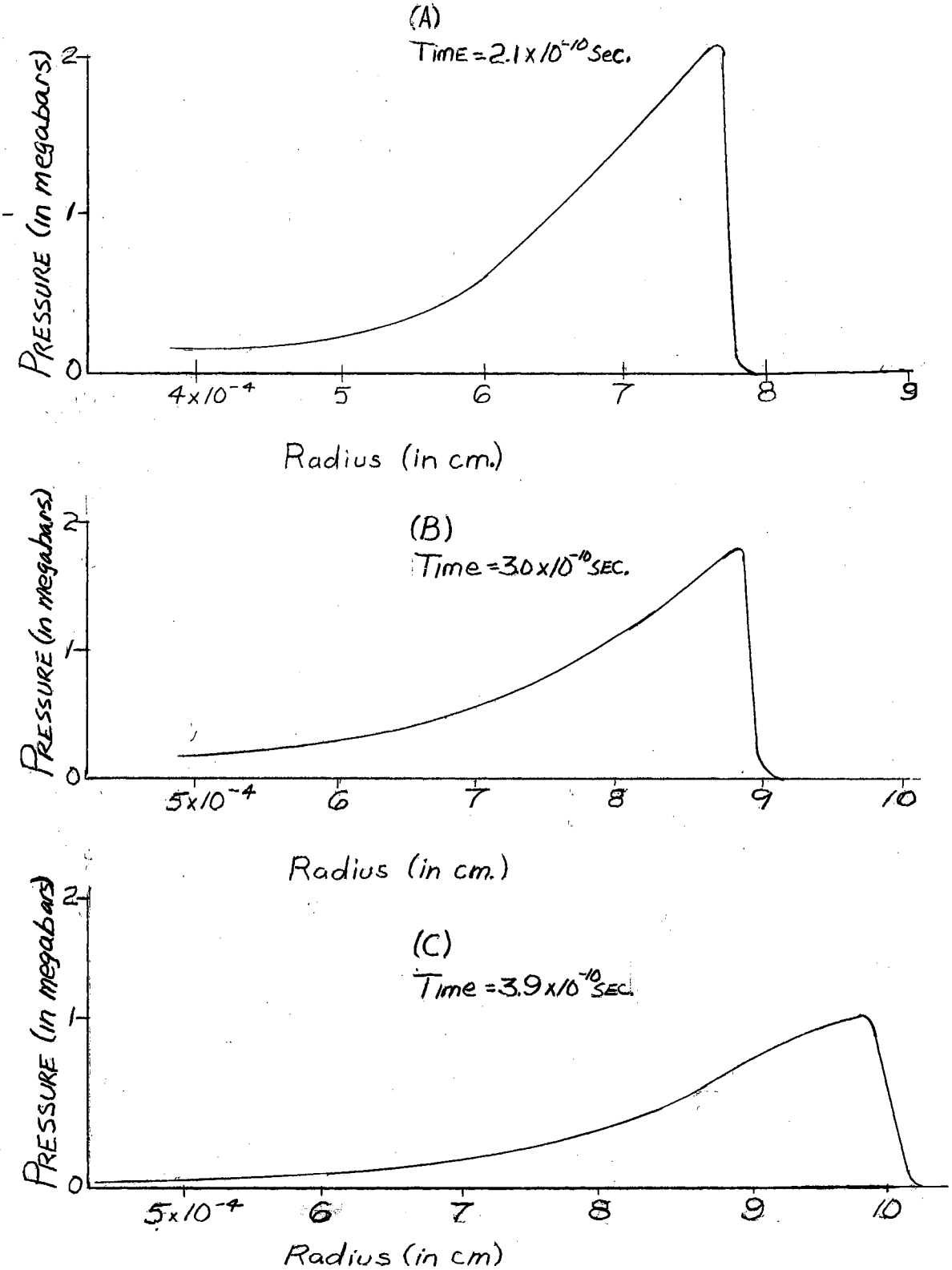

FIGURE 8 PRESSURE PROFILES AT
$T = 2.1 \times 10^{-10}$, 3.0×10^{-10}, AND 3.9×10^{-10} SECONDS

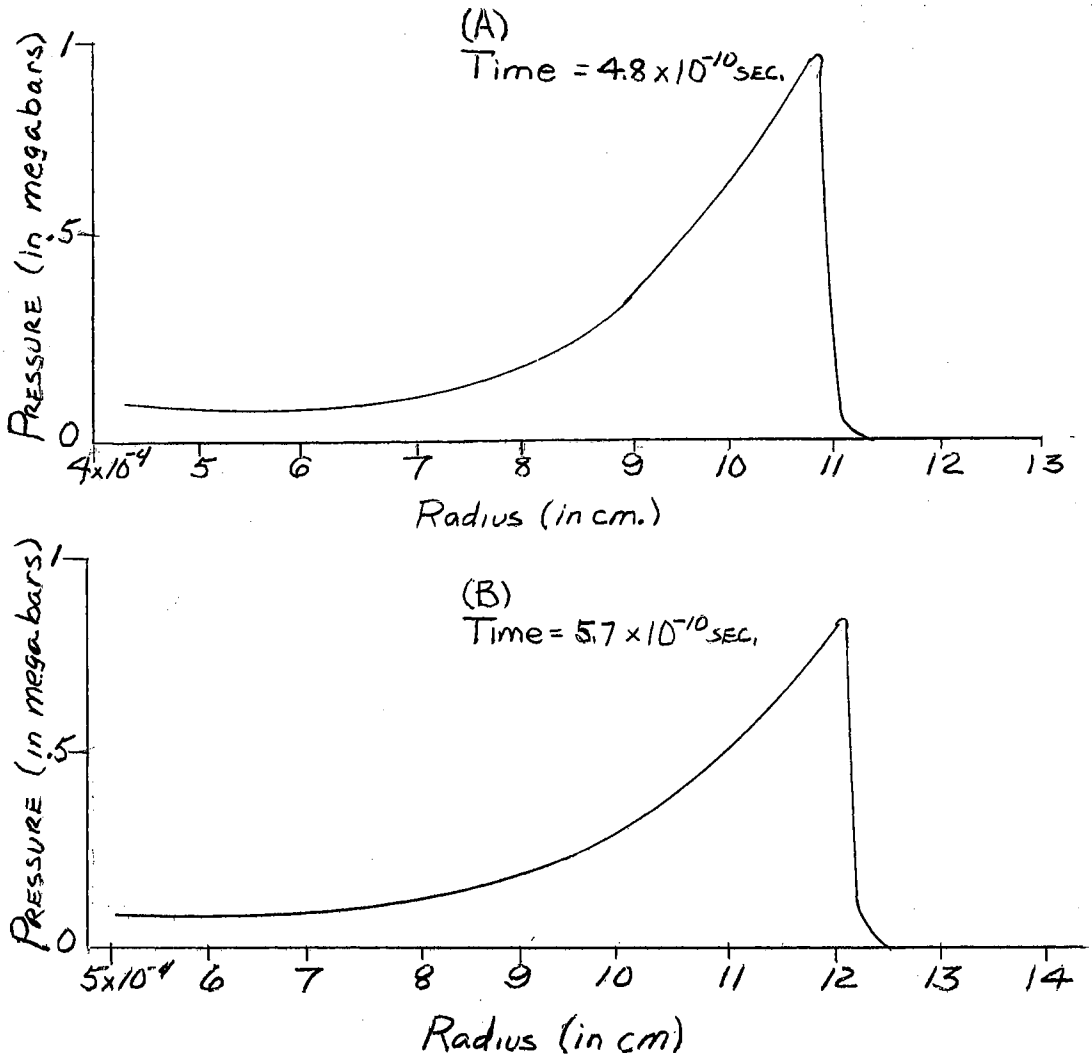

FIGURE 9 PRESSURE PROFILES AT
$T = 4.8 \times 10^{-10}$, 5.7×10^{-10}, 6.5×10^{-10} SECONDS.

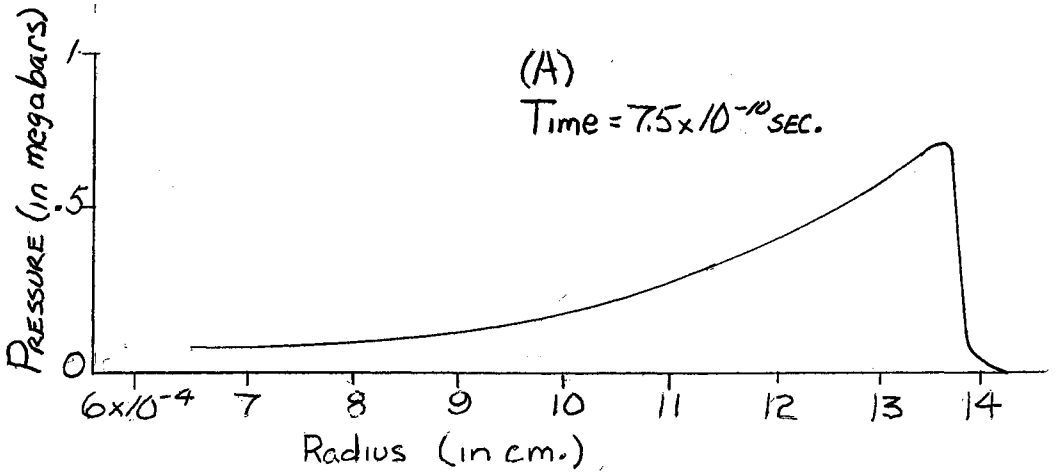

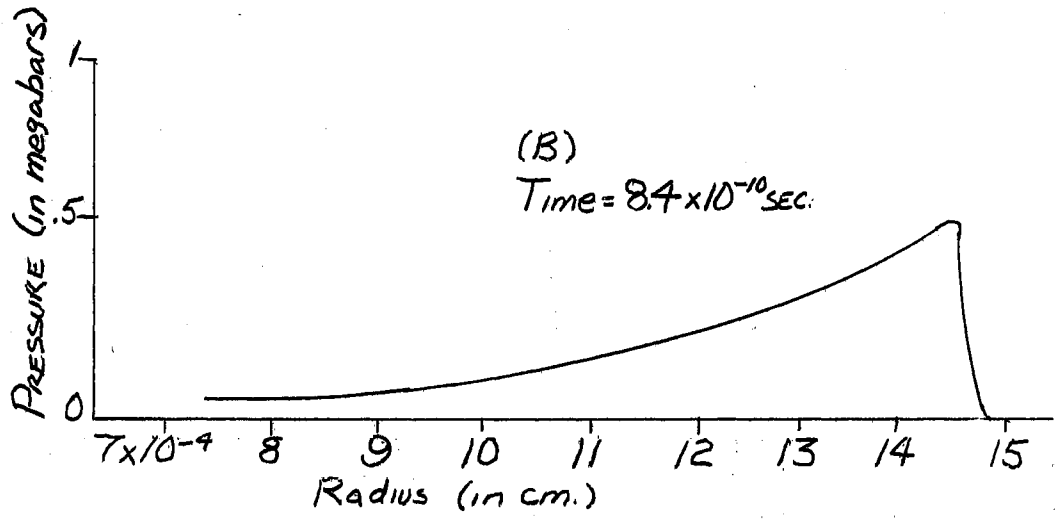

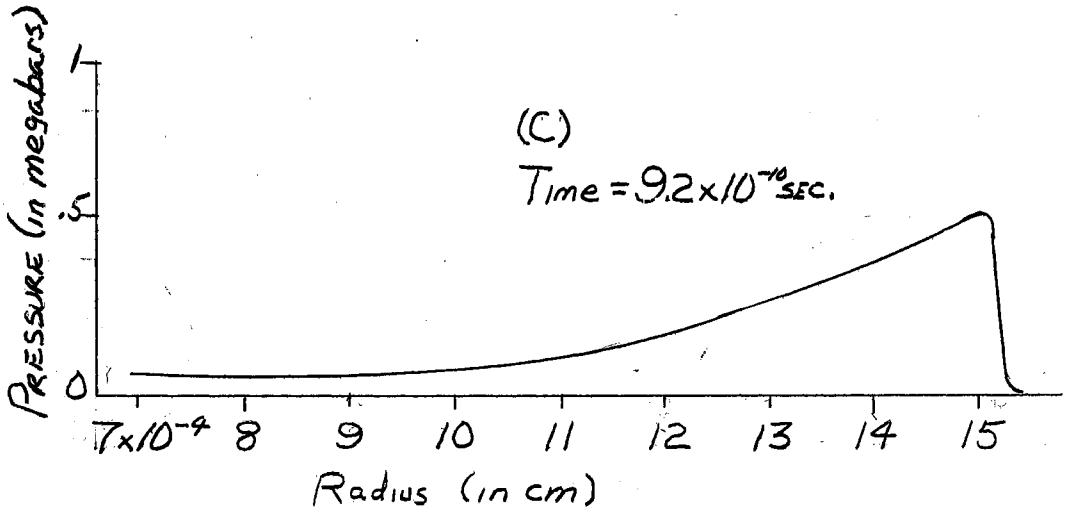

FIGURE 10 PRESSURE PROFILES AT
$T = 7.5\times10^{-10}$, 8.4×10^{-10}, 9.2×10^{-10} SECONDS

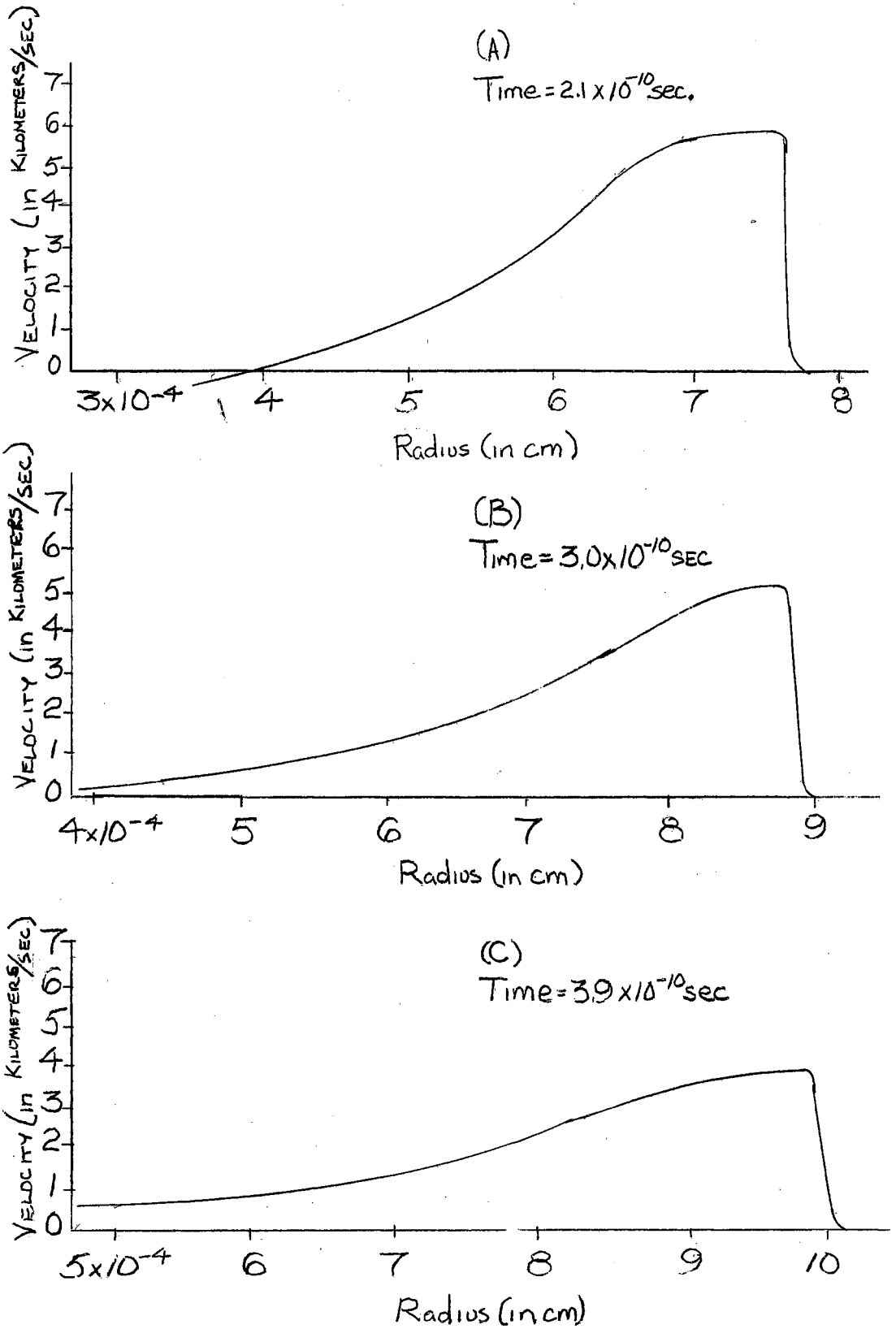

FIGURE 12 VELOCITY PROFILES AT $T = 2.1 \times 10^{-10}$, 3.0×10^{-10}, AND 3.9×10^{-10} SECONDS

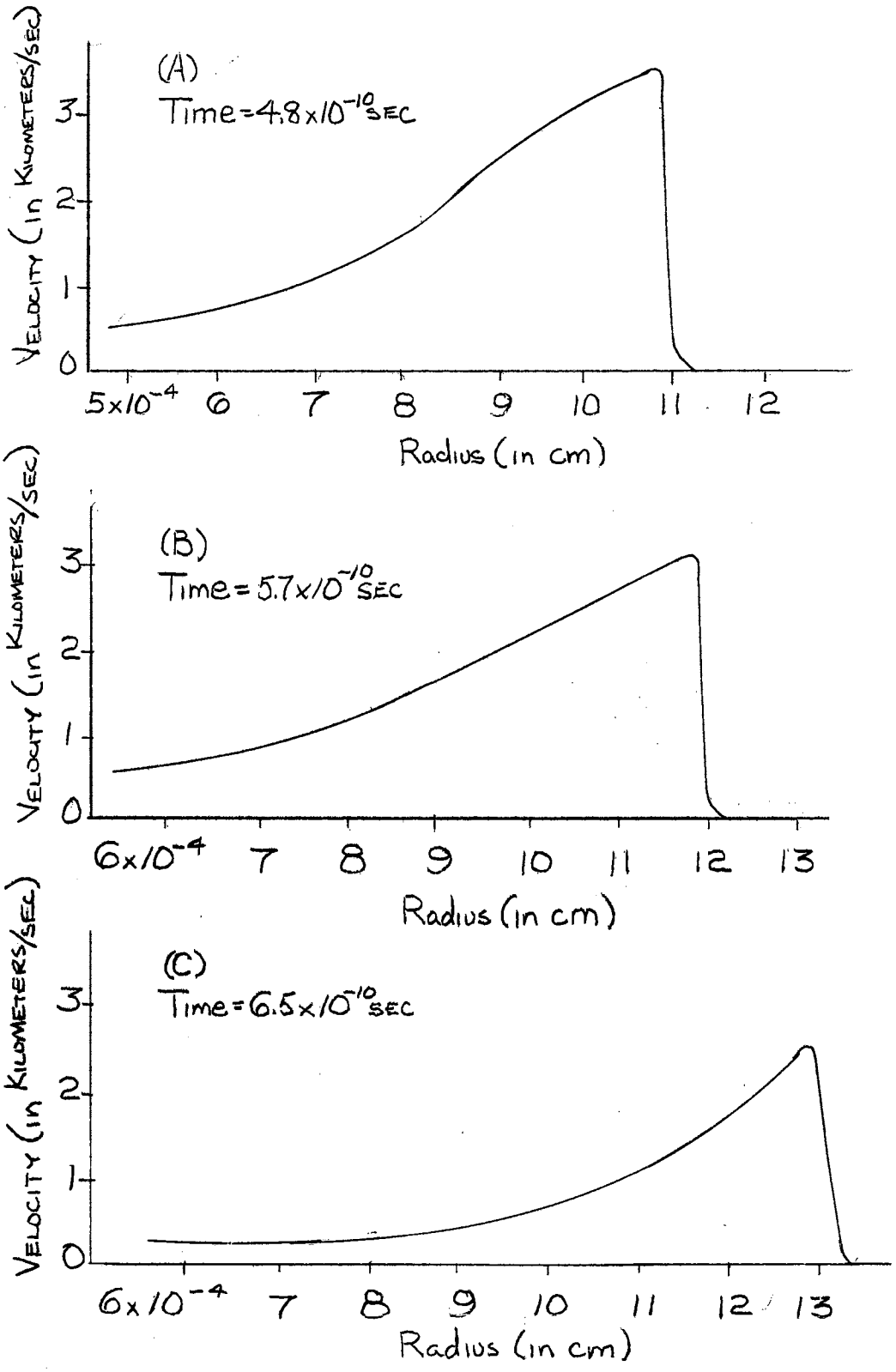

FIGURE 13 VELOCITY PROFILES AT $T = 4.8 \times 10^{-10}$, 5.7×10^{-10}, AND 6.5×10^{-10} SECONDS

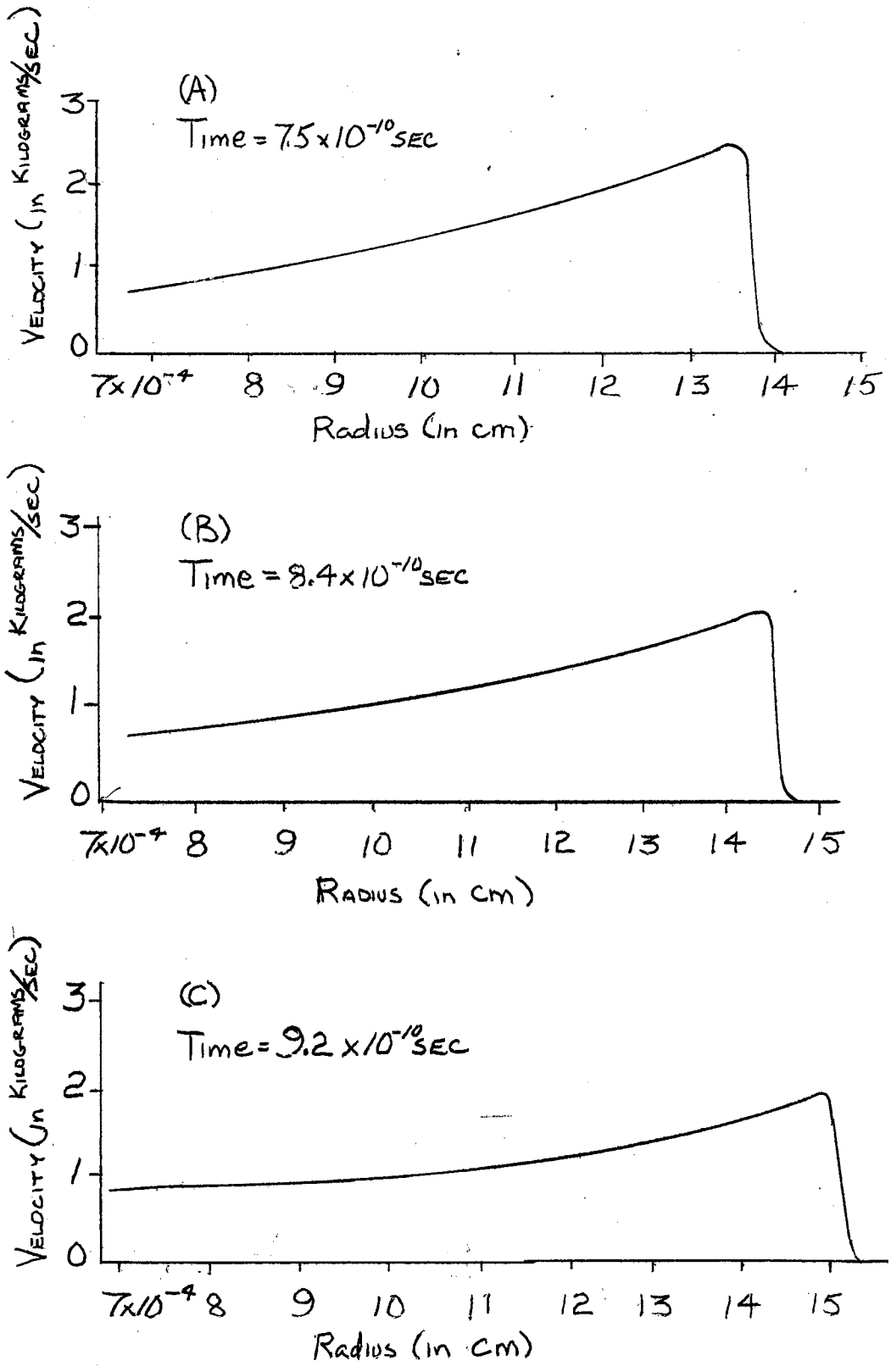

FIGURE 14 VELOCITY PROFILES AT

$T = 7.5 \times 10^{-10}$, 8.4×10^{-10}, AND 9.2×10^{-10} SECONDS

meteoroid. This condition existed for a very short time and then reversed in sign as is shown in Figure (12b), indicating that the material is again flowing radially outward from the point of impact.

Profiles of relative density corresponding to the pressure and velocity solutions are presented in Figures (15), (16), (17), and (18). The term relative is the density behind the shock front, relative to that of the undisturbed material ahead of the shock. It is noted that the density behind the shock wave drops to a value less than its original value. This is to be expected since one of the assumptions governing hydrodynamic flow given in Chapter IV is that flow is adiabatic behind the shock. The compression-expansion cycle of the aluminum target can be explained with the aid of Figure (19), a plot of adiabats crossing the Hugoniot at various pressure levels.

The material undergoing shock is raised to the peak pressure of the shock wave along the locus of pressure-volume points described by the Hugoniot Relation. After the shock wave moves forward, the material starts to expand adiabatically. Thus the material drops towards its original pressure along the adiabat which intersects the Hugoniot Curve at the peak pressure of the shock wave. It is noted from Figure (17) that adiabats intersecting the Hugoniot at relatively high pressures will not intersect the relative specific volume axis until $V/V_o > 1$ or $\rho/\rho_o < 1$. Therefore the material that has undergone shock compression drops to a relative density of less than unity.

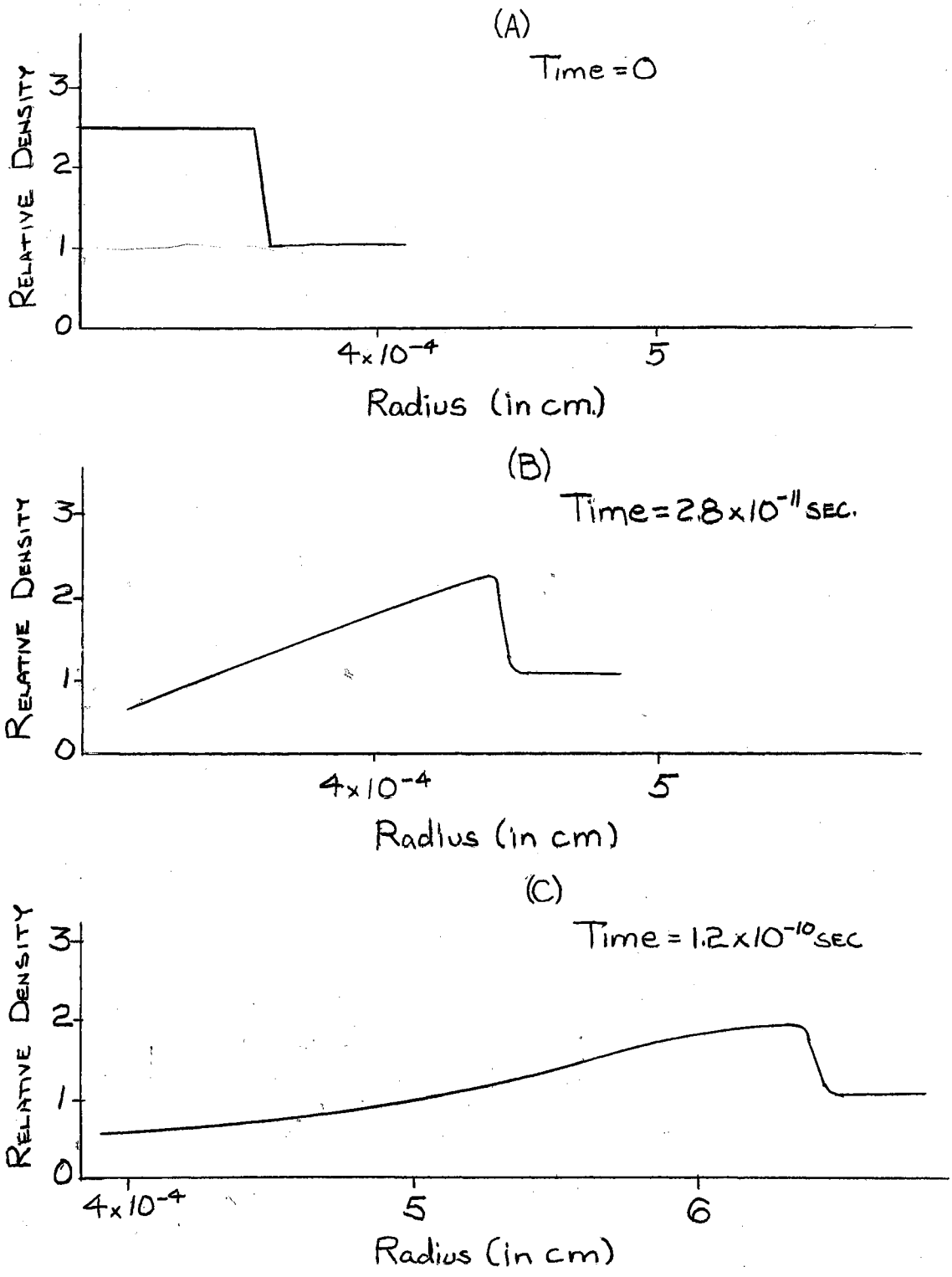

FIGURE 15 RELATIVE DENSITY PROFILES AT $T=0$, 2.8×10^{-11}, AND 1.2×10^{-10} SECONDS

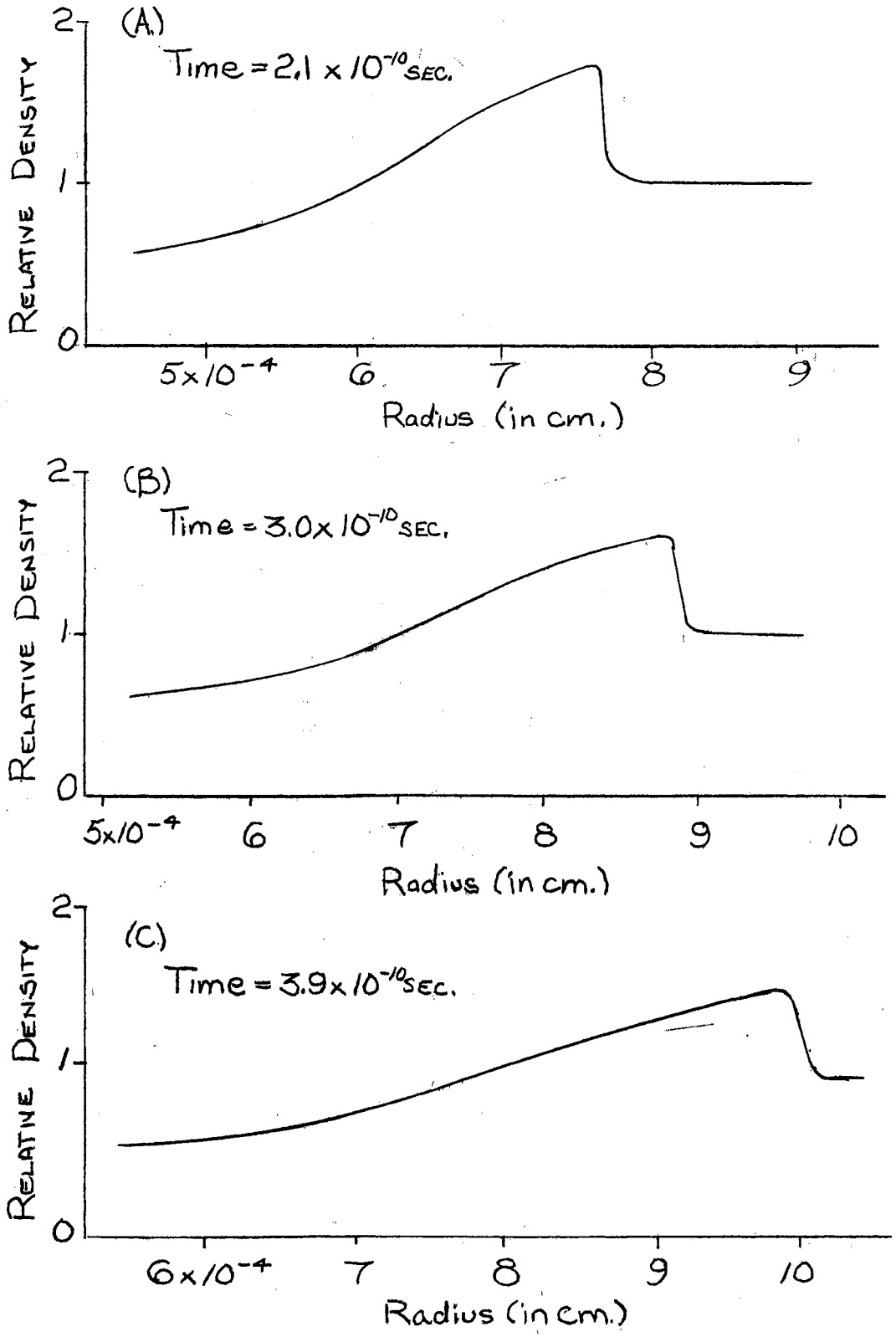

FIGURE 16 RELATIVE DENSITY PROFILES AT $T = 2.1 \times 10^{-10}$, 3.0×10^{-10}, AND 3.9×10^{-10} SECONDS

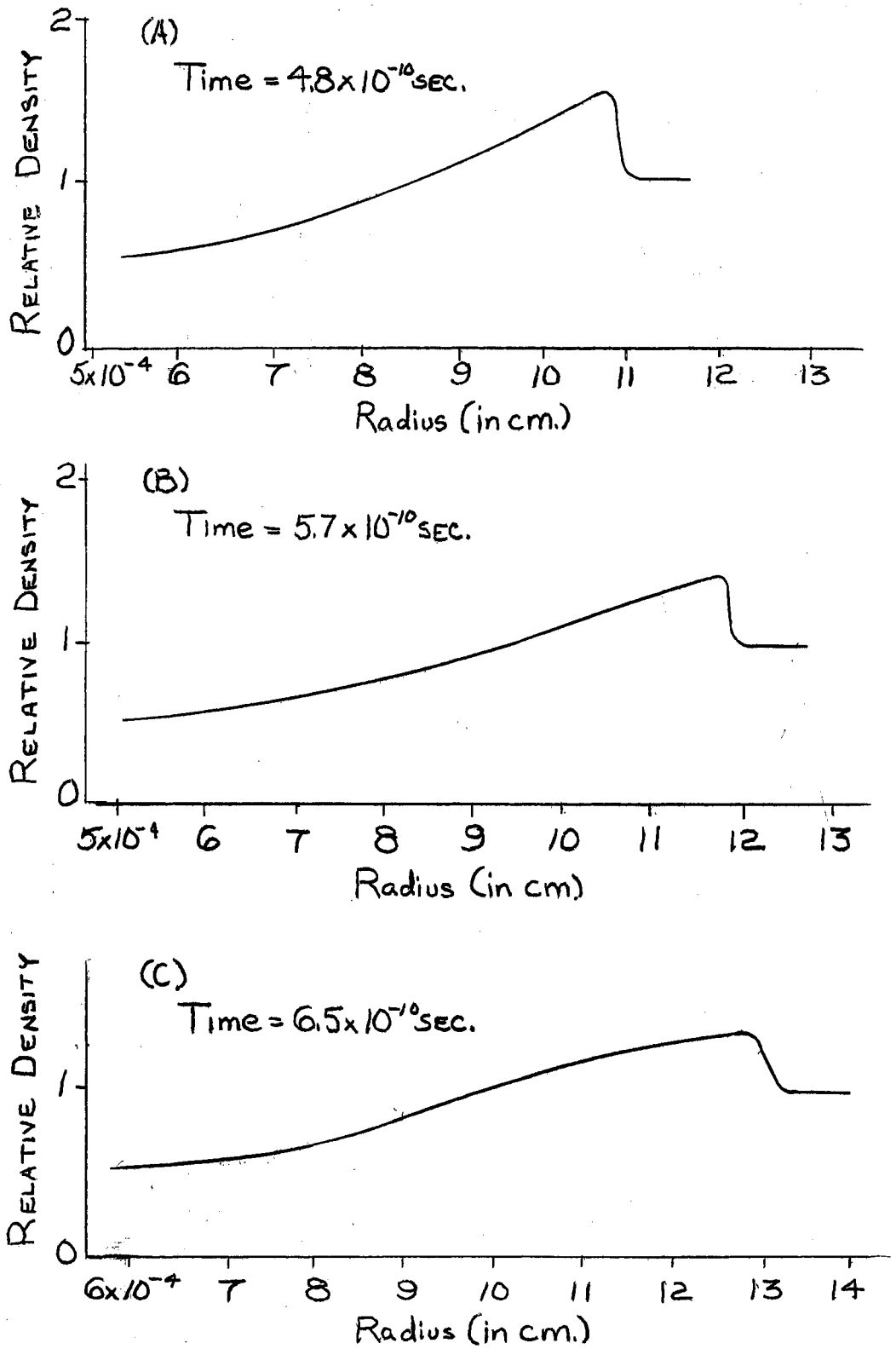

FIGURE 17 RELATIVE DENSITY PROFILES AT $T = 4.8 \times 10^{-10}$, 5.7×10^{-10}, AND 6.5×10^{-10} SECONDS

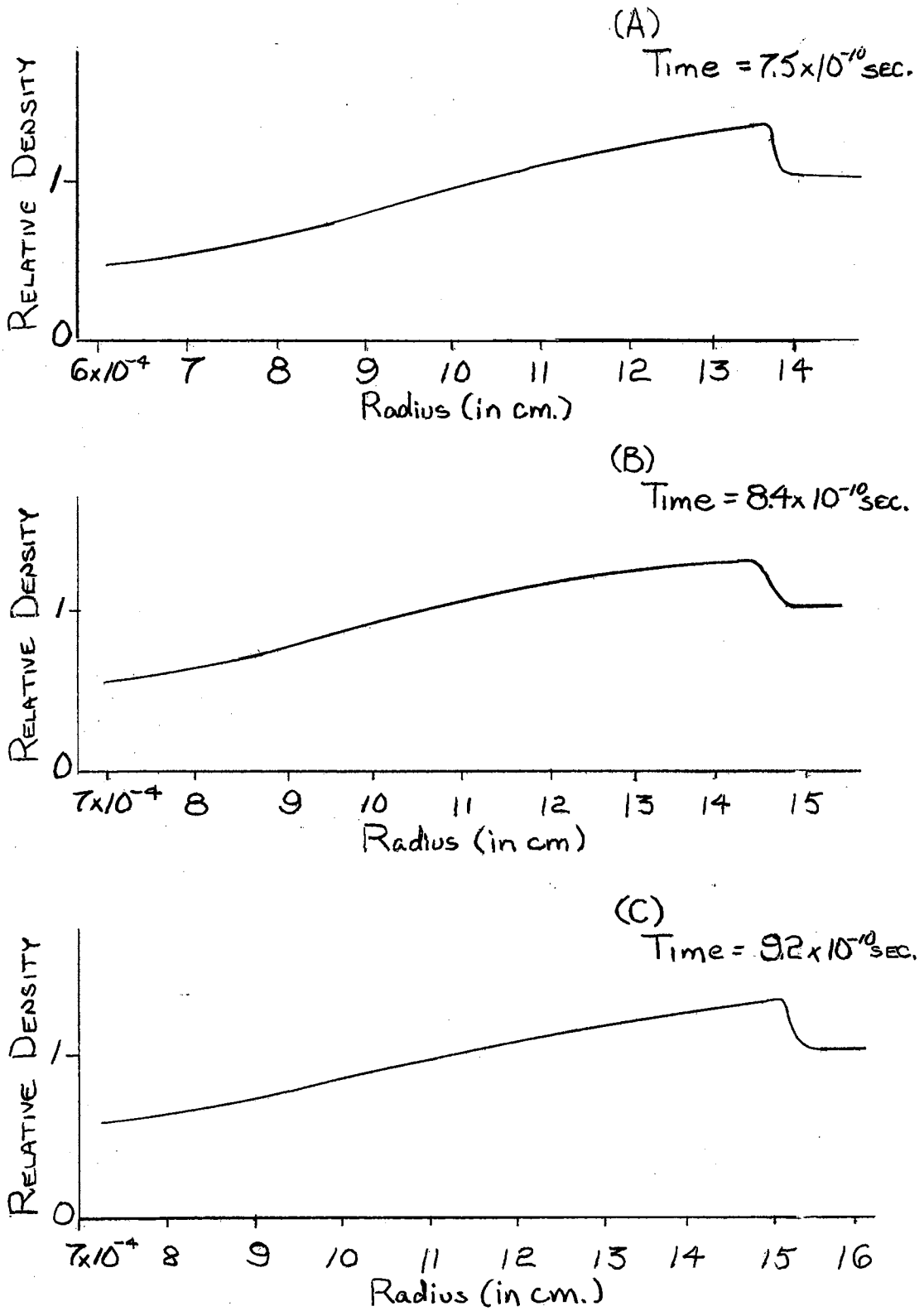

FIGURE 18 RELATIVE DENSITY PROFILES AT $T = 7.5 \times 10^{-4}$, 8.4×10^{-4}, AND 9.2×10^{-10} SECONDS

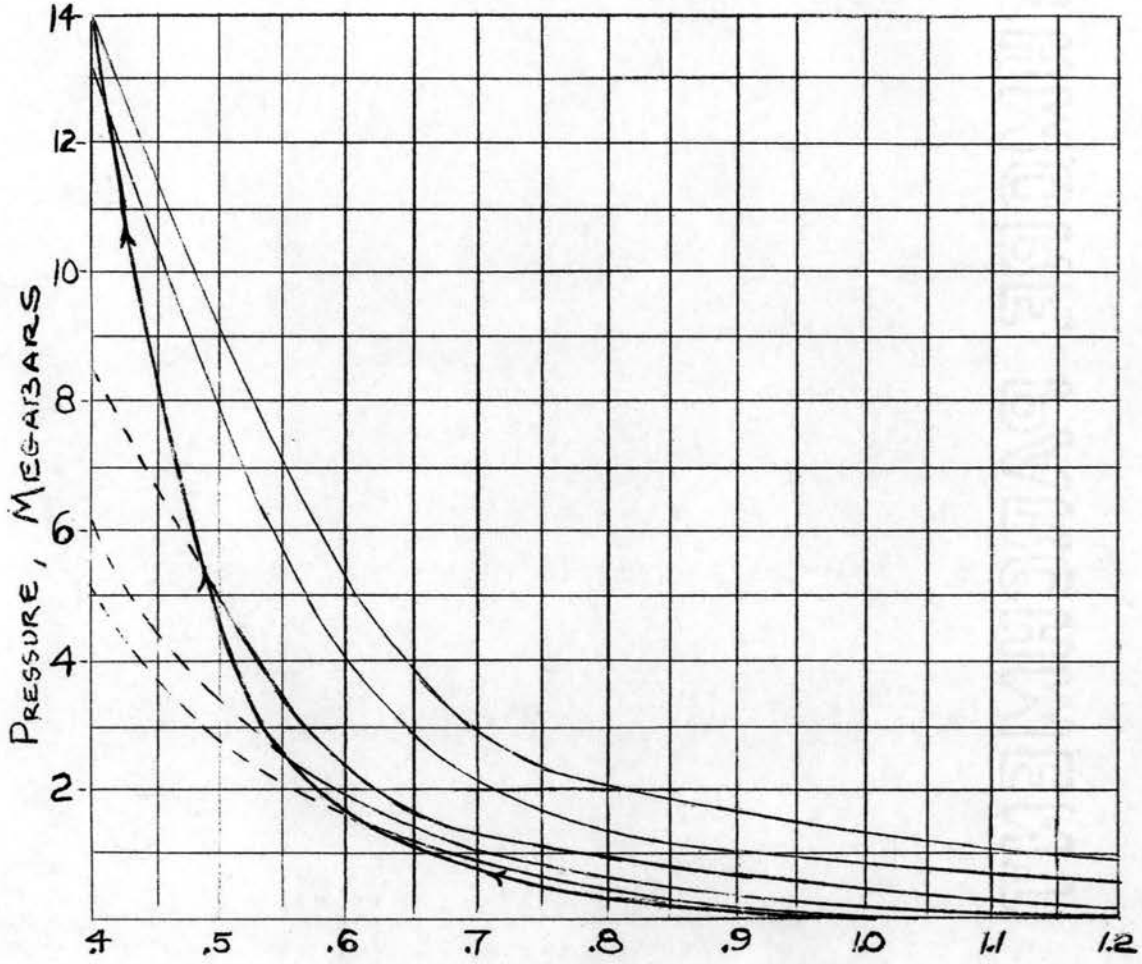

SEVERAL ADIABATS ARE SHOWN INTERSECTING AT 14.1, 12.6, 5.3, 2.4 AND 1.4 MEGABARS.

FIG. 19 ADIABATS CROSSING THE HUGONIOT

CHAPTER VII

SUMMARY AND CONCLUSIONS

The solution for the propagation of a spherical shock wave into a semi-infinite solid has been obtained in this thesis. A method was employed that was developed and proved for the solution of shock waves in gases or fluids. The equations and the computer program are sufficiently versatile to solve any spherical shock with arbitrary initial and boundary conditons. This particular problem was simplified to permit solution on a computer with a limited memory. While it is realized that this simplified version is only an order of magnitude approximation to the true impact problem, the solution of such a problem is required to provide the basis for better assumptions which are necessary to treat more complex problems on a larger, faster digital computer. This first approximation permits parameters, such as the coefficient of the dissipative mechanism and the space-time net, to be determined for the dimensions that are involved in the solution of micrometeoroid impact. The machine solution has been followed until the peak pressure of the shock wave is only 3.5% of the initial value.

Recommendations for Future Work

The next logical step in the study of the shock wave associated with micrometeoroid impact could be the solution of a

two dimensional shock propagating into a layered media. This problem will probably require that the hydrodynamic equations be solved in the Eulerian form on a digital computer somewhat larger and faster than the IBM 650. Also, the problem should include the development of initial conditions and boundary conditions that more correctly describe the mechanisms of impact than those used for the first approximation which is solved in this thesis.

SELECTED BIBLIOGRAPHY

1. Collins, Rufus D., Jr. and William Kinard, NASA TN D-230, May, 1960.

2. Cook, M. A. "Mechanism of Cratering in Ultra-High Velocity Impact", J. Appl. Phys. 30 (1959) 725-735.

3. Hamann, S. D. Physico-Chemical Effects of Pressure. New York: Academic Press (1957) 57-60

4. Bethe, H. A. OSRD No. 545, Division B of National Defense Research Committee "The Theory of Shock Waves for an Arbitrary Equation of State".

5. von Neumann, J. and R. D. Richtmyer. J. Appl. Phys. 21 (1950) 232-237.

6. Courant, R. and K. O. Friedrichs. Supersonic Flow and Shock Waves. New York: Interscience Publishers (1948) p. 118.

7. l. c. 6, p. 119.

8. l. c. 6, p. 134.

9. l. c. 6, p. 123.

10. Walsh, J. M., N. H. Rice, R. G. McQueen and F. L. Yarger. Phys. Rev. 108, (1957) 196.

11. Rice, N. H., R. G. McQueen and J. M. Walsh. Solid State Physics, Advances in Research and Applications. New York: Academic Press (1958) 1-63.

12. Latter, Richard. Phys. Rev., 99 (1955) 1854.

13. Latter, Richard. Jour. Chem. Phys., 24 (1955) 280.

14. l. c. 6, p. 140.

15. Scarborough, J. B. Numerical Mathematical Analysis 2nd Ed. Baltimore: John Hopkins Press (1950)

16. Bjork, R. L. "Effects of a Meteoroid Impact on Steel and Aluminum in Space". Engineering Division, RAND Corporation, P-1662 (1958) 3

17. l. c. 6, p. 12.

18. Lamb, Horace. Hydrodynamics 6th Ed. Chapter I, Cambridge: Cambridge Press, (1932).

19. Richtmyer, R. D. Difference Methods of Initial-Value Problems. New York: Interscience Publishers (1957) 189.

20. Sokolnikoff, I, S., and R. M. Redheffer. Mathematics of Physics and Modern Engineering. New York: McGraw-Hill Book Company, Inc. (1958) 417.

21. l. c. 6, p. 15.

22. l. c. 19, p. 192.

23. l. c. 19, p. 199.

24. l. c. 19, p. 207.

25. l. c. 19, p. 208.

26. l. c. 19, p. 210.

27. Brode, H. S. J. Appl. Phys., 26, (1955) 766-775.

28. Milne, W. E. Numerical Solution of Differential Equations. New York: John Wiley and Sons (1953).

29. Thomas, L. H. Numerical Solution of Partial Differential Equations of Parabolic Type. Seminar on Scientific Computation. International Business Machines Corp. (1949).

30. Peaceman, D. W. and H. H. Rachford, Jr. "The Numerical Solution of Parabolic and Elliptic Differential Equations". J. Soc. Industrial and Appl. Math., 3 (1955) 28.

31. Lax, P. D. and R. D. Richtmyer. "Survey of the Stability of Linear Finite Difference Equations". Communications Pure and Appl. Math. 9 (1956) 267.

32. Slater, John C. and N. H. Frank. Mechanics. New York: McGraw-Hill Book Company, Inc. (1947) 230.

33. l. c. 19, p. 216

34. l. c. 19, p. 221.

35. Charters, A. C. Scientific American, 203 (October, 1960) 128-140.

36. Todd, F. C. and H. R. Lake. "Analytical and Limited Experimental Study of the Mechanisms of Impact, Penetration and Light Emission for Micrometeorites on an Aluminum-Coated Photomultiplier". Quarterly Progress Report, No. 1. NASr-7, Research Foundation, Oklahoma State University, December 31, 1960.

37. l. c. 11, p. 47.

38. Bridgeman, P. W. Proc. Am. Acad. Arts and Sci., 77 (1949) 189; 76 (1948) 55; 76 (1945) 9; 74 (1945) 425.

39. Zaker, T. A. Point Source Explosion in a Solid. AEC Research and Development Report. Contract No. AT(11-1)-528, (1959).

40. l. c. 39, p. 10.

41. l. c. 39, p. 9.

APPENDIX A

IMPACT THEORY

In a recently published article in the Scientific American (35), it is shown that the depth of penetration of a projectile impinging on the surface of a block of material varies in a strange manner. In Figure (20) the variation in depth of penetration with velocity is shown for a tungsten carbide pellet which impinges on a lead block. The curve can be divided into three regions with respect to the velocity. In the first region, the depth of penetration increases linearly with an increase in velocity. The projectile remains unbroken in this region and the penetration is believed to result from a shear mechanism. In the second region, labled the transition region, a phenomena other than shearing starts to take place. The depth of penetration now varies more slowly with a change in velocity. In the third region, labeled fluid impact, the penetration is a cratering phenomena. That is, the hole that is left in the material is a crater of nearly hemispherical shape.

It is the third region that is of the most interest for micrometeoroid impact.

Thermal Damage Theory

Some have proposed that penetration in the fluid region can

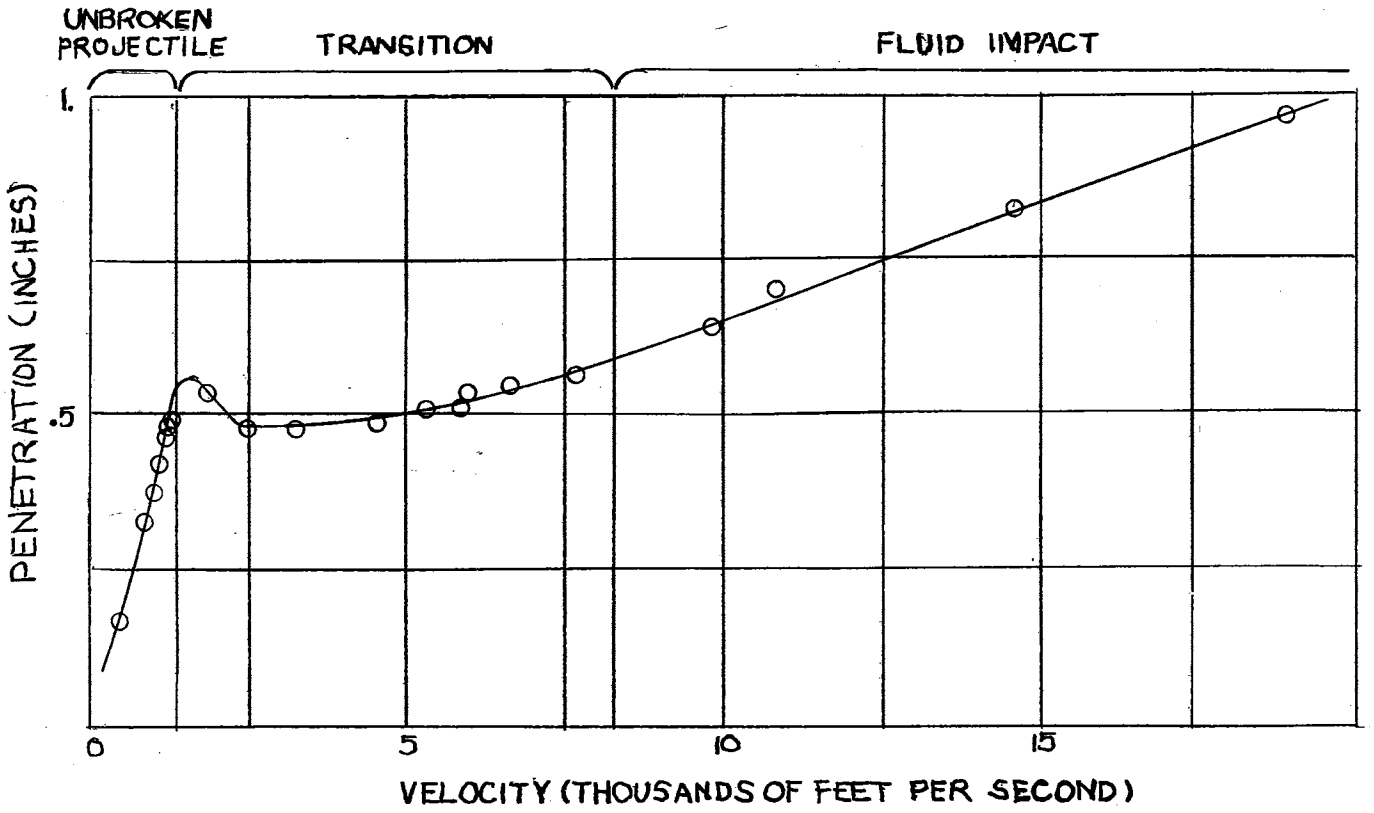

FIG. 20. PENETRATION DEPTH VERSUS PROJECTILE VELOCITY

be explained by a thermal damage theory (2). This theory predicts that the mechanisms of impact produce sufficient energy density to vaporize the projectile and target material. Production of light observed upon impact is attributed to incandescence of the target material.

The thermal damage model is not accepted entirely in this thesis for the following reasons. First, it is known from experiment that when the phenomena of cratering starts to take place, the projectile no longer retains a form that resembles its original shape. The crater that is produced is found to be lined with the projectile material. The thermal model, however, does not offer any explanation for this lining effect. Conversely, it would seem that when the target material was converted to a vapor, the projectile material should also be converted to a vapor and the explosion of the hot vapor into its surroundings should throw the projectile material out of the crater.

A second reason for not accepting the entire thermal damage model is suggested from examinations of a limited amount of high velocity impact data (1). An investigation was made of the volume of the crater in an aluminum target. The total kinetic energy per unit mass of the projectile was computed and plotted against the energy necessary to heat the mass of aluminum that would fill the equivalent volume of the crater from room temperature to the melting point of aluminum. It can be seen from Figure (21) that at the highest projectile energy observed it would take 70 per cent of the input energy simply to heat and melt the volume of aluminum that is removed from the crater. This assumes

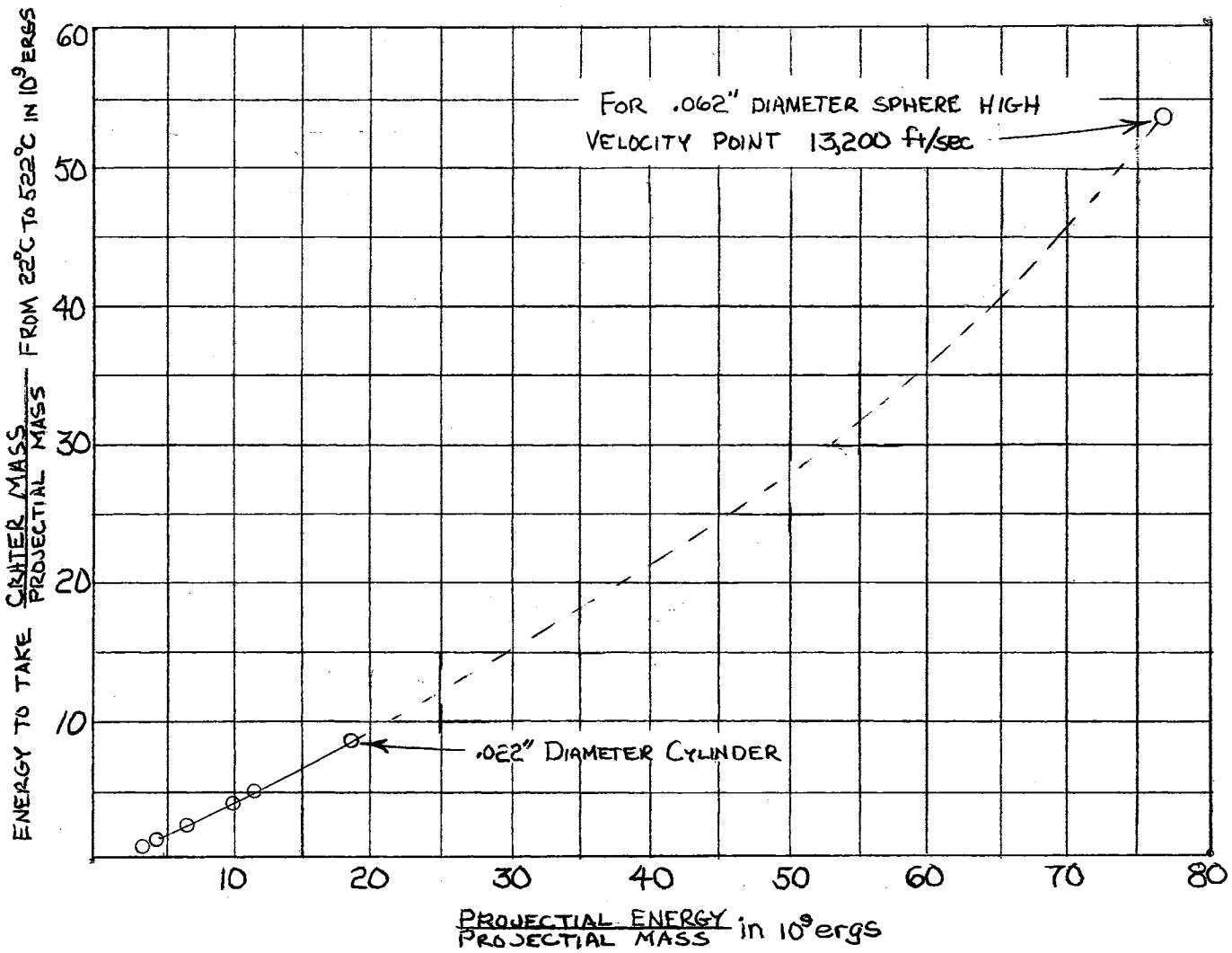

FIG. 21., RELATIVE ENERGY OF PROJECTILE VERSUS RELATIVE ENERGY NEEDED TO HEAT CRATER MASS TO BOILING POINT.

that no energy goes into melting the projectile. Therefore, very little energy is left to be radiated and none to supply the latent heat to vaporize a substantial part of the material. Also, the volume removed would take more of the kinetic energy if it were to be converted to a high density vapor. It is also shown in Figure (21) that at velocities that are barely in the cratering velocity region it takes at least 50 per cent of the impact energy to melt the equivalent volume of aluminum. This investigation is substantiated by a picture in the Scientific American article by Charters (35). Here the volume of the cavity in copper was measured by the scaling given in the picture and the measurements reveal that 50 per cent of the projectile energy is necessary to heat and melt the crater volume of copper in the crater. Since such an appreciable amount of the incident energy is necessary to melt the material in the crater it seems that a more plausiable explanation of the impact phenomena must be offered. Another possible mechanism of impact that has been given consideration is the hydrodynamic model.

Hydrodynamic Model of Impact

The hydrodynamic model of ultra-high velocity impact suggests that the penetration of the projectile into the target is much the same as one fluid penetrating another. That is, the target and projectile under the tremendous forces of impact become plastic and the plastic projectile penetrates the plastic target. The hemispherical shape of the crater is attributed to a strong radial shock accompanying penetration.

The most apparent failure of the hydrodynamic model is that it does not include a mechanism for the production of light. An acceptable model must include a radiation mechanism.

This model also fails to predict other observed phenomena. To successfully explain the projectile material being evenly distributed over the crater surface, it would be necessary for the plastic projectile material to be held together by some type of force such as a surface tension. For this problem, the forces involved are much greater than any known cohesive forces. Calculations for the typical micrometeoroid with a velocity of 36 kilometers per second indicate that the energy involved would correspond to an iron "gas" ion with each atom having an energy of 376 electron-volts (36). There are no known cohesive forces which differentiate between materials with a value of the energy as great as two per cent of this energy. Finally, the hydrodynamic model does not predict a change in penetration phenomena for increase in projectile velocity as is depicted in Figure (20).

Failure of the thermal damage and hydrodynamic models to account for all of the observed phenomena associated with ultra-high velocity impact makes necessary the proposal of still another impact model.

Proposed Plasma Impact Model

The model of impact proposed by this study group differs from other proposed models most radically in the mechanism of the projectile material penetration. After the initial contact of the micrometeoroid and the target, the pressure for a very short time will have a tremendous magnitude. Under these tremendous forces

it will be impossible for the projectile and target material to remain in their crystaline form. The two materials are probably converted to plasmas (a mixture of ions and electrons) when the impact pressure reaches approximately 100,000 atmosphere (3). The penetration mechanism for this model can be described as the interaction of two dissimilar plasmas, with one penetrating the other. The plasma from the meteoroid will flow through the plasma of the target material. It is also proposed that a radial shock wave would account for the nearly hemispherical shape of the crater that is formed by the impact of an ultra-high velocity projectile. It may be noted at this point that the proposed model partially agrees with the assumptions made in both the thermal damage and hydrodynamic models of impact. The plasma model includes a radial shock which was assumed to accompany the hydrodynamic model and it also assumes that the material in the immediate vicinity of impact has a high energy density as does the thermal model. It differs from the thermal damage model in that for thermal damage, the high energy density is in the form of a high temperature; whereas, for the plasma model more of the energy is in the form of recoverable potential energy.

It is readily seen that radiation from the thermal damage model will be of a different form than that of the plasma model. The thermal damage model must radiate black-body radiation which is a continuous spectrum. A plasma would emit radiation in lines which may be broadened by associated microfields. The light that would be emitted by an aluminum plasma would be in the far ultra-

violet and extend into the visible. Therefore, far ultra-violet spectrometry of radiation produced by high-velocity impact will yield an experimental check of the existance of plasma.

APPENDIX B

THE MIE-GRUNEISEN EQUATION OF STATE

The Mie-Gruneisen equation of state can be derived from consideration of the total energy of a fluid of interest (11). Assume that the thermal energy of a fluid can be described by a set of simple harmonic oscillators whose frequencies are ν_α . The internal energy may be expressed as follows,

$$E = \Phi + \sum_{\alpha=1}^{3N} \tfrac{1}{2} h\nu_\alpha + \sum_{\alpha=1}^{3N} \frac{h\nu_\alpha}{\exp[h\nu_\alpha/KT] - 1} \qquad \alpha = 1,2,\cdots 3N \tag{1}$$

where K is Boltzman's constant, h is Planck's constant, N is the number of atoms and the summation is made over the 3N normal modes. The symbol Φ represents the potential energy of the fluid with the atoms in a state of equilibrium. The Helmholtz free energy for this model is,

$$A = \Phi + \sum_{\alpha=1}^{3N} \tfrac{1}{2} h\nu_\alpha + KT \sum_{\alpha=1}^{3N} \ln(1-\exp[-h\nu_\alpha/KT]) \tag{2}$$

Recalling that the pressure is equal to the partial derivative of the Helmholtz free energy with respect to the volume M for a constant temperature, the pressure for this model may be written:

$$P = -\frac{d\Phi}{dV} + \frac{1}{V} \sum_{\alpha=1}^{3N} \gamma_\alpha \left[\tfrac{1}{2} h\nu_\alpha + \frac{h\nu_\alpha}{\exp[h\nu_\alpha/KT] - 1} \right] \tag{3}$$

where γ_α is defined as,

$$\gamma_\alpha = - \frac{d(\ln \upsilon_\alpha)}{d(\ln V)}$$

At this point the approximation is made that all γ_α's are equal. Then equation (3) can be rewritten in the form,

$$P = - \frac{d\Phi}{dV} + \frac{\gamma}{V} \sum_{\alpha=1}^{3N} \tfrac{1}{2} h\upsilon_\alpha + \frac{h\upsilon_\alpha}{\exp[h\upsilon_\alpha / KT] - 1} = \frac{d\Phi}{dV} + \frac{\gamma}{V} e_{vib} \qquad (4)$$

where e_{vib} is the vibrational energy of the fluid and the assumption is made that Gruneisen's Ratio, $\gamma(V)$, is a function of the volume only. The terms in equation (4) can be rearranged into the following form,

$$P - \left[- \frac{d\Phi}{dV} + \frac{\gamma}{V} \sum_{\alpha=1}^{3N} \tfrac{1}{2} h\upsilon_\alpha \right] = \frac{\gamma}{V} \sum_{\alpha=1}^{3N} \frac{h\upsilon_\alpha}{\exp[h\upsilon_\alpha / KT] - 1} \qquad (5)$$

If the temperature, T, in equation (3) is allowed to approach zero, it is seen that the pressure along the zero degree isotherm may be expressed as,

$$P_k = - \frac{d\Phi}{dV} + \frac{\gamma}{V} \sum_{\alpha=1}^{3N} [\tfrac{1}{2} h\upsilon_\alpha] \qquad (6)$$

The right side of equation (5) is equal to $\frac{\gamma}{V}$ times the thermal contribution of the internal energy so that it may be rewritten:

$$P - P_k = \frac{\gamma}{V}(e - e_k) \qquad (7)$$

where P_k and e_k are the pressure and internal energy along the zero degree isotherm.

This is one form of the Mie-Gruneisen equation of state. It

can be written in terms of any P, V, and e curve so that in terms of the Hugoniot curve, equation (7) can be written

$$P - P_h = \frac{\gamma}{V} (e - e_k) \tag{8}$$

Since a P, V, e equation of state is desired, the pressure and the internal energy along the Hugoniot must be expressed as functions of the specific volume for equation (7) to be in the proper form. Rice, et.al., (11) obtained an experimental Hugoniot curve for aluminum by a method discussed in Appendix C. They fit a cubic polynomial to their experimental Hugoniot data for which the pressure along the Hugoniot equals a function of the volume, which is

$$P_h = P_h(V)$$

Remembering the Hugoniot relation, equation (18) from Chapter II,

$$e_h - e_o = \tfrac{1}{2}(P_h + P_o) \cdot (V_o - V_h)$$

where P_o, V_o, and e_o are the pressure, specific volume and specific internal energy ahead of the shock front and P_h, V_h, and e_h are the pressure, specific volume, and specific internal energy behind the shock. This relation may be rewritten in the form

$$e_h = \tfrac{1}{2}(P_h + P_o) \cdot (V_o - V_h) + e_o \tag{9}$$

By considering $P_h = P_h(V)$, the internal energy along the Hugoniot, e_h, is a function of the volume, $e_h = e_h(V)$.

Thus equation (8) can be rewritten,

$$P - P_h(V) = \frac{\gamma(V)}{V}\left(e - e_h(V)\right) \tag{10}$$

The Mie-Gruneisen equation in this form is a complete P, e, V equation of state. It is applicable to the pressure range over which the Hugoniot is known as a function of the volume, within the bounds of the approximation that Gruneisen's Ratio may be approximated by a function of only one variable, the volume.

The Gruneisen Ratio

The approximation for Gruneisen's Ratio, γ, that is used in this treatment of the equation of state is the Dugdale-MacDonald relation:

$$\gamma = -\frac{V}{2}\left[\frac{\frac{\partial^2 (PV^{2/3})}{\partial V^2}}{\frac{\partial (PV^{2/3})}{\partial V}}\right] - \frac{1}{3} \tag{11}$$

The justification of the approximations is supported by work of McQueen, et.al., (11).

For the present treatment of a high pressure equation of state, it is possible to consider the pressure ahead of the shock equal to zero since

$$P_o \ll P_h$$

Using this approximation, equation (7) may be rewritten,

$$P - P_k = \frac{\gamma}{V}\left(e + \int_{V_o}^{V} P_k dV\right)$$

since

$$e_k = -\int_{V_o}^{V} P_k dV$$

By considering the pressure and specific internal energy along the Hugoniot, equation (7) may be rewritten,

$$P_h - P_k = \frac{\gamma}{V}\left[\tfrac{1}{2}P_h(V_o - V) + e_o + \int_{V_o}^{V} P_k dV\right] \tag{12}$$

and γ may be expressed in the following relation

$$\gamma = \tfrac{1}{2}P_h(V_o - V) + e_o \int_{V_o}^{V} P_k dV \tag{13}$$

It is seen from equation (13) that γ can be solved for any value of the variable, V, if the values of P_h and P_k are known functions of the volume.

It should be observed at this point that there is not good agreement in the literature on the value of γ at high pressure. It is fortunate however, that errors up to 25% in γ lead to uncertainties that are no larger than those introduced by considering experimental curves of the Hugoniot (37).

APPENDIX C

EXPERIMENTAL HUGONIOT

The method described in this appendix for determining the pressure-compression curves for solids depends upon the measurement of two variables. These two variables, the free surface velocity of a plate supporting a shock wave and the shock velocity in the plate, have been measured by a method (10) devised by J. M. Walsh and associates.

Two methods are used to convert the measured velocities to pressure-compression points. Both depend on the Rankine-Hugoniot jump conditions that express the conservation of mass and the conservation of momentum. These two equations may be written in the form,

$$(1)\quad \frac{V}{V_o} = (U_s - U_p)/U_s \qquad \text{Conservation of Mass}$$

$$(2)\quad P = \rho_o U_s U_p + P_o \qquad \text{Conservation of Momentum}$$

Here V and P are the pressure and the specific volume behind the shock wave, P_o, V_o, ρ_o are the pressure, specific volume, and the density ahead of the shock wave. U_s, U_p are the velocity of the shock wave and of the particle velocity behind the shock wave.

The first method of determining the pressure-compression

points depends upon an approximation of the free surface velocity. The measured free surface velocity is due to two factors. It is due in part to the particle velocity, U_p, behind the shock wave and it is due in part to a rarefacation wave with a velocity, U_r, which relieves the pressure at the free surface. The approximation is made that $\frac{U_r}{U_p} = 1$. This approximation can be used with the equation that the free surface velocity, U_{fs}, equals the sum of the particle velocity, U_p, and the rarefacation wave velocity, U_r, to show the particle velocity is approximately equal to one-half the measured free surface velocity. Then with the measured free surface velocity, the measured shock velocity, and equations (1) and (2), it is possible to directly compute the volume ratio, $\frac{V}{V_o}$, and the pressure P for a given shock wave. Thus by varying the strength of the shock wave, it is possible to plot a Hugoniot pressure-compression curve.

The second method for converting shock velocity to pressure-compression data is a graphical method which uses a graph of the pressure versus particle velocity and equation (2) to find the pressure and particle velocity. The particle velocity and the measured shock velocity are then used with equation (1) to find the volume ratio, $\frac{V}{V_o}$.

The data that is obtained by either of these two methods is analytically fit to an equation of the following form:

$$P_h = A\mu + B\mu^2 + C\mu^3 \qquad (3)$$

Where P_h represents pressure on the Hugoniot curve and

$$\mu = \left(\frac{V_o}{V} - 1\right) = \left(\frac{\rho}{\rho_o} - 1\right)$$

Here ρ and ρ_o are the densities behind and in front of the shock respectively, and

A, B, and C are constant determined by the shape of the experimental Hugoniot.

The constants for 24ST aluminum were determined by Rice, et.al., and they are,

A =765, B =1659, and C =428

for the pressure, P_h, in kilobars. The data obtained for 24ST aluminum are illustrated in Figure (22). In this figure, the experimental Hugoniot is plotted. In addition, the bounding zero degree isotherm, and the adibats that cross the bottom and the top of the Hugoniot are plotted. Walsh, et.al., did not extend their data below 100 kilobar. However, the isotherms for aluminum below 100 kilobar was experimentally determined by Bridgemann, (38) and the analytical fit by Walsh of P_h includes data points determined by him.

From the Hugoniot relation,

$$e_h - e_o = \tfrac{1}{2}(P_h + P_o) - (V_o - V)$$

it is possible to write an expression for the specific internal energy along the Hugoniot in terms of the specific volume. Assume that the pressure ahead of the shock wave, P_o, to be zero, then the internal energy expression may be written as follows,

$$e_h - e_o = \frac{A\mu^2 + B\mu^3 + C\mu^4}{2\rho_o(\mu + 1)} \qquad (4)$$

This form of the Hugoniot is used in the Mie-Gruneisen equation of state for the problem solved in this thesis.

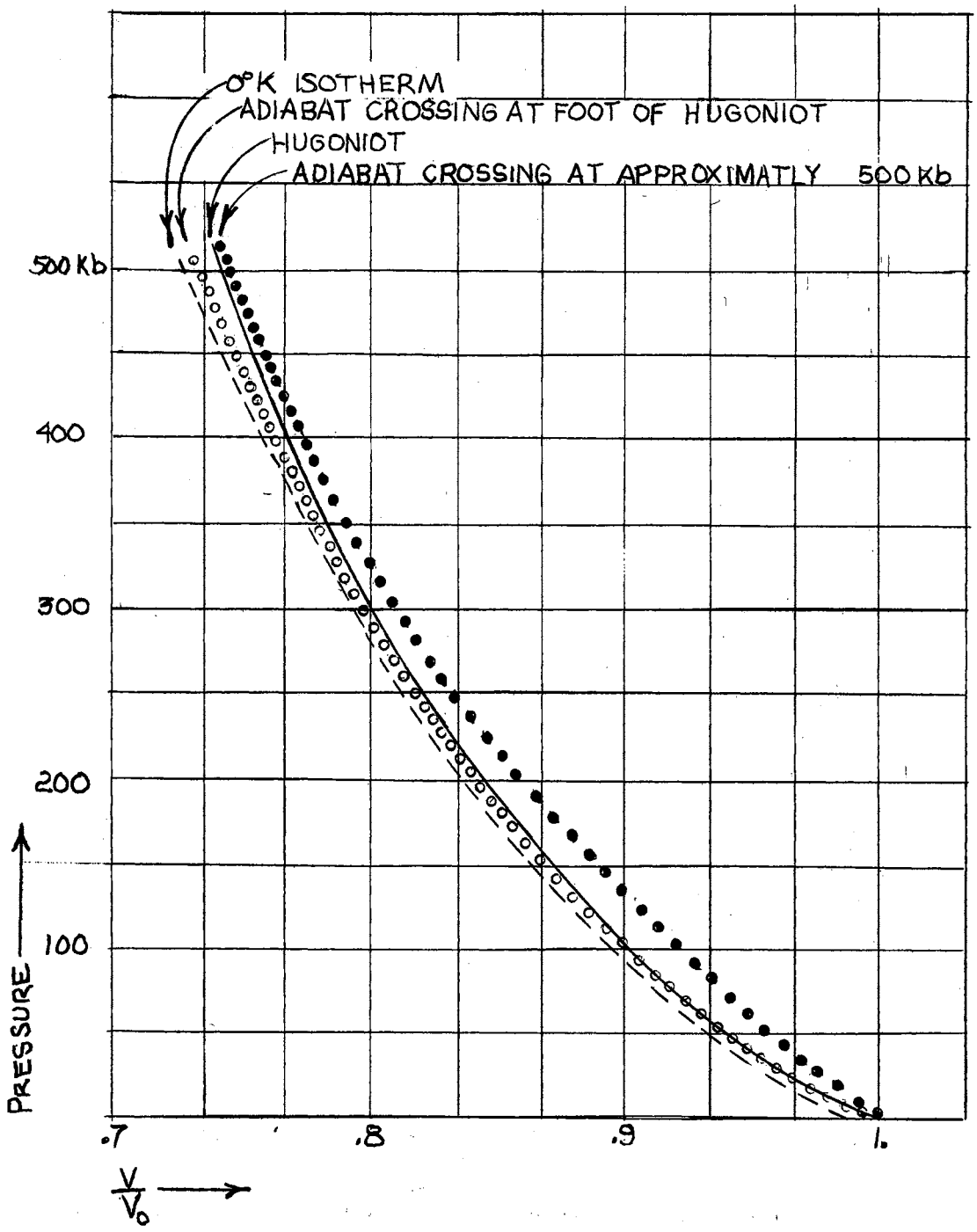

FIG. 22. EXPERIMENTAL HUGONIOT

APPENDIX D

CALCULATION OF INITIAL VALUES

This appendix will set forth the iterative method derived by Mr. J. G. Ables for calculation of initial values which exist for the model of impact described in Chapter VI. The method is derived from the following conditions and equations:

1. Conservation of momentum between the micrometeoroid and target material.
2. Conservation of energy between the micrometeoroid and target material.
3. The Rankine-Hugoniot conditions.
4. The Hugoniot curve, $P_h = A\mu + B\mu^2 + C\mu^3$

The assumptions that are made for this derivation are,

1. The micrometeoroid is a sphere of diameter, 6.2×10^{-4} cm.; mass, 10^{-9} gram; density 8.0; and velocity 3.6×10^{6} cm/sec.
2. The micrometeoroid is perfectly rigid and has penetrated one-half of its diameter into the target.
3. Impact produces a strong radial shock in the aluminum which has a hemispherical front centered on the point of contact.
4. The values of the pressure, density, and flow velocity between the interface and the shock front are constant.
5. The kinetic energy, potential energy, and pressure in front of the shock are zero.
6. The flow of aluminum behind the shock front is radially outward from the point of initial contact.

Symbols that are used in the derivation are defined as follows,

follows,

V =Specific volume of the compressed target material.

V_o =Initial specific volume of the target material.

P_h =Hugoniot pressure.

E =Total kinetic and potential energy of the compressed material.

E_o =Total kinetic energy of the micrometeoroid before impact.

E_T =Kinetic energy of the compressed target material.

E_r =Kinetic energy of the micrometeoroid after it has penetrated a depth of one-half of its diameter into the target.

V_o =Initial velocity of micrometeoroid before impact.

V_r =Residual velocity of the micrometeoroid after the indicated penetration.

$D = \frac{V_r}{V_o}$

V_m =Total volume of micrometeoroid.

ρ_o =Initial density of target material.

ρ =Density of compressed target material.

ρ_m =Density of micrometeoroid.

r_m =Radius of micrometeoroid.

r_s =Radius of shock compressed target material.

$R = \frac{r_s}{r_m}$

W_o =Initial momentum of micrometeoroid after impact.

W_r =Residual momentum of micrometeoroid after impact.

W_s = Momentum of shock compressed target material.

m = Mass of the micrometeoroid.

The conservation of energy between the micrometeoroid and the target material may be expressed as,

$$E_o = E + E_r \tag{1}$$

Zaker (39) in his work on a point explosion in a solid, shows that the total energy of the compressed material is equal to twice its kinetic energy. Therefore, equation (1) may be written,

$$E_o = 2E_T + E_r \tag{2}$$

Using the symbols defined in this appendix, conservation of momentum may be expressed as,

$$W = W_r + W_s \tag{3}$$

The equations for conservation of energy and conservation of momentum may be combined by remembering that the kinetic energy of a mass is equal to one-half the square of the momentum divided by the mass. Thus the kinetic energy of the compressed material can be written as,

$$E_T = \frac{(\frac{1}{2})W_s}{(2/3)\Pi\rho(r_s^3 - r_m^3)} \tag{4a}$$

or,

$$E_T = \frac{3W_s^2}{\Pi\rho(r_s^3 - r_m^3)} \tag{4b}$$

The density, ρ, of the compressed material is equal to the mass of the material contained in a hemisphere of radius r_s before impact divided by the volume of the compressed hemispherical shell of target material after impact. Thus,

$$\rho = \frac{(2/3)\Pi r_s^3 \rho_o}{(2/3)(r_s^3 - r_m^3)} \tag{5a}$$

or

$$\rho = \frac{\rho_o r_s^3}{r_s^3 - r_m^3} \tag{5b}$$

Using the value of ρ from equation (5b), equation (4b) may be rewritten,

$$E_T = \frac{3W_s^2}{\Pi \rho_o r_s^3} \tag{6}$$

This allows the conservation of energy, equation (1) to be expressed as,

$$E_o = \frac{6W_s^2}{\Pi \rho_o r_s^3} + E_r \tag{7}$$

The radius cubed, r_s^3, may be obtained from equation (7) as,

$$r_s^3 = \frac{6W_s^2}{\Pi\rho_o(E_o - E_r)} \tag{8}$$

which allows the ratio, $R^3 = \frac{r_s^3}{r_m^3}$, to be formed,

$$R^3 = \frac{6W_s^2}{\Pi\rho_o r_m^3(E_o - E_r)} \tag{9}$$

By substituting the value of W_s from equation (3) into equation (9) and remembering that the mass, m, of the micrometeoroid can be expressed as,

$$m = \rho_m(r/3)\Pi r_m^3$$

equation (9) can be rewritten,

$$R^3 = \frac{8(W_o - W_r)^2}{m(E_o - E_r)} \cdot \frac{\rho_m}{\rho_o} \tag{10}$$

The dimensionless quantities Q_o and Q_1 are defined as,

$$Q_o = \frac{E_o - E_r}{E_o}$$

and

$$Q_1 = \frac{W_o - W_r}{W_o}$$

Using these dimensionless variables, the value of R^3 from equation (10) is,

$$R^3 = \frac{8}{m} \cdot \left(\frac{\rho_m}{\rho_o}\right) \cdot \left(\frac{Q_1^2}{Q_o}\right) \cdot \left(\frac{W_o^2}{E_o}\right) \tag{11}$$

It is noted that,

$$\frac{W_o^2}{E} = 2m$$

since the kinetic energy of the micrometeoroid is equal to one-half the square of the momentum divided by the mass. Therefore, equation (11) may be written,

$$R^3 = 16\left(\frac{\rho_m}{\rho_o}\right) \cdot \frac{Q_1^2}{Q_o} \tag{12}$$

If the dimensionless quantity, $\frac{Q_1^2}{Q_o}$ is examined, it is noted that,

$$\frac{Q_1^2}{Q_o} = \frac{(W_o - W_r)^2}{E_o - E_r} \cdot \frac{E_o}{W_o^2} \tag{13a}$$

or

$$\frac{Q_1^2}{Q_o} = \frac{(W_o - W_r)^2}{2m(E_o - E_r)} \tag{13b}$$

From the relationship between kinetic energy and momentum, $E_o - E_r$ may be expressed as,

$$E_o - E_r = \frac{W_o^2 - W_r^2}{2m} \tag{14}$$

Using the value of $E_o - E_r$ from equation (14), equation (13b) may be written,

$$\frac{Q_1^2}{Q_o} = \frac{(W_o - W_r)^2}{W_o^2 - W_r^2} \tag{15a}$$

or,

$$\frac{Q_1^2}{Q_o} = \frac{\left(1 - \frac{W_r}{W_o}\right)^2}{1 - \left(\frac{W_r}{W_o}\right)^2} \tag{15b}$$

If W_o and W_r are written in the form,

$$W_o = \tfrac{1}{2}(mv_o^2)$$

and

$$W_r = \tfrac{1}{2}(mv_r^2)$$

Equation (15b) may be rewritten as,

$$\frac{Q_1^2}{Q_o} = \frac{\left(1 - \frac{v_r}{v_o}\right)^2}{1 - \left(\frac{v_r}{v_o}\right)^2} \tag{16a}$$

or, using the notation $D = \frac{v_r}{v_o}$

$$\frac{Q_1^2}{Q_o} = \frac{(1 - D)^2}{(1 - D^2)} \tag{16b}$$

This expression for $\frac{Q_1^2}{Q_o}$, allows equation (12) to be written,

$$R^3 = 16\frac{\rho_m}{\rho_o}\frac{(1 - D)^2}{(1 - D^2)} \tag{17}$$

The ratio of the specific volume, V, of the compressed target material, to the specific volume, V_o, of the target material before impact may be formed as,

$$\frac{V}{V_o} = \frac{(2/3)\ \Pi\left(r_s^3 - r_m^3\right)}{(2/3)\ \Pi\ r_s^3} \tag{18a}$$

or

$$\frac{V}{V_o} = \left(1 - \frac{1}{R^3}\right) \tag{18b}$$

Taking the value of R^3 to be that expressed as in equation (17), equation (18b) is rewritten,

$$\frac{V}{V_o} = 1 - \frac{\rho_o}{16\rho_m} \cdot \frac{1 - D^2}{(1 - D)^2} \tag{19}$$

This is the first equation of the set to be used in the iterative calculation of the initial values.

The second equation used in the iterative scheme is the

Hugoniot equation,

$$P_h = A\mu + B\mu^2 + C\mu^3 \qquad (20)$$

$$\text{where } \mu = \frac{V_o}{V} - 1$$

discussed in Chapter III.

The third equation of the iteration set is a modified form of the Hugoniot relation,

$$\frac{\Delta E}{\Delta V} = \tfrac{1}{2}(P_1 + P_o) \qquad (21)$$

also discussed in Chapter III.

The quantities ΔE and ΔV are the change in internal energy of the target material due to impact compression, and the change in specific volume respectively. For the model being considered, ΔE is equal to one-half of the total energy of the compressed material (40) and ΔV is one-half the micrometeoroid volume, V_m. Remembering the assumption that the pressure ahead of the shock wave is zero, equation (21) can be written,

$$E = \tfrac{1}{2} V_m P_h \qquad (22)$$

The final equation making up the iterative set is equation (1),

$$E = E_o - E_r \qquad (1)$$

written in the form,

$$E = E_o \left[1 - \frac{\frac{1}{2}(mv_r^2)}{\frac{1}{2}(mv_o^2)} \right] \qquad (23a)$$

or

$$E = E_o(1 - D^2) \tag{23b}$$

The iterative method for solving the initial pressure and specific volume of the compressed material may be stated as follows.

1. Choose a value of D such that $0 \leq D < L$
2. Compute $\frac{V}{V_o}$ from equation (19)

$$\frac{V}{V_o} = 1 - \frac{\rho_o}{16\rho_m} \cdot \frac{1 - D^2}{(1 - D)^2}$$

3. Compute P_h from equation (20)

$$P_h = A\mu + B\mu^2 + C\mu^3 \quad \text{where } \mu = \frac{V_o}{V} - 1$$

4. Compute E from equation (22)

$$E = \tfrac{1}{2}V_m P_h$$

5. Compute E from equation (23b)

$$E = E_o(1 - D)^2$$

6. Compare the value of E computed in step 5 with that computed in step 4.
   a. $E_4 - E_5 > 0$, decrease D and return to step 2.
   b. $E_5 - E_4 > 0$, increase D and return to step 2.
   c. $E_5 = E_4$, the correct values of P_h and $\frac{V}{V_o}$ have been obtained.

The method described was programmed for solution on the

IBM 650 by Mr. B. A. Sodek and Mr. J. G. Ables.

When the correct values of P_h and $\frac{V}{V_o}$ have been obtained, the proper value of the flow velocity is solved for by an equation derived from the Rankine-Hugoniot relations by Zaker (41).

$$u^2 = P_h(V_o - V) \tag{24}$$

This equation gives the flow velocity that is needed to satisfy the Rankine-Hugoniot condition across the shock and complete the calculation of initial values.

VITA

Harry Russell Lake

Candidate for the Degree of

Master of Science

Thesis: DIGITAL COMPUTER SOLUTION FOR PROPAGATION OF A SPHERICAL SHOCK WAVE IN ALUMINUM

Major Field: Physics

Biographical:

Personal Data: Born at Stillwater, Oklahoma, May 9, 1937, the son of Delbert O. and Agnes M. Lake.

Education: Attended grade school at Greenfield, Oklahoma, graduated from Greenfield High School in 1955; received the Bachelor of Science degree from Oklahoma State University, with a major in Physics, in May, 1959.

Professional Experience: Employed by Diamond Ordnance Fuze Laboratory for summer in 1960; employed as a Graduate Assistant in the Oklahoma State University Physics Department while completing graduate studies.